AFML-TR-76-56
PART I

IMPACT RESISTANCE OF STRUCTURAL CERAMICS PART I: INSTRUMENTED DROP-WEIGHT TESTS

PROCESSING AND HIGH TEMPERATURE MATERIALS BRANCH
METALS AND CERAMICS DIVISION

MAY 1976

TECHNICAL REPORT AFML-TR-76-56 PART I
REPORT FOR PERIOD JUNE 1975 - FEBRUARY 1976

AIR FORCE MATERIALS LABORATORY
AIR FORCE WRIGHT AERONAUTICAL LABORATORIES
AIR FORCE SYSTEMS COMMAND
WRIGHT-PATTERSON AIR FORCE BASE, OHIO 45433

NOTICE

When Government drawings, specifications, or other data are used for any purpose other than in connection with a definitely related Government procurement operation, the United States Government thereby incurs no responsibility nor any obligation whatsoever; and the fact that the government may have formulated, furnished, or in any way supplied the said drawings, specifications, or other data, is not to be regarded by implication or otherwise as in any manner licensing the holder or any other person or corporation, or conveying any rights or permission to manufacture, use, or sell any patented invention that may in any way be related thereto.

This report has been reviewed by the Information Office (OI) and is releasable to the National Technical Information Service (NTIS). At NTIS, it will be available to the general public, including foreign nations.

This technical report has been reviewed and is approved.

JAMES M. WIMMER
Project Scientist

FOR THE COMMANDER

NORMAN M. TALLAN
Acting Chief, Processing and High
Temperature Materials Branch
Metals and Ceramics Division
Air Force Materials Laboratory

Copies of this report should not be returned unless return is required by security considerations, contractual obligations, or notice on a specific document.

UNCLASSIFIED

SECURITY CLASSIFICATION OF THIS PAGE (When Data Entered)

REPORT DOCUMENTATION PAGE

READ INSTRUCTIONS BEFORE COMPLETING FORM

1. REPORT NUMBER: AFML-TR-76-56-Pt-I	2. GOVT ACCESSION NO.
3. RECIPIENT'S CATALOG NUMBER	
4. TITLE (and Subtitle): Impact Resistance of Structural Ceramics. Part I. Instrumented Drop-Weight Tests.	5. TYPE OF REPORT & PERIOD COVERED: Interim Report. June 75-Feb 76
	6. PERFORMING ORG. REPORT NUMBER
7. AUTHOR(s): I. Bransky, J. M. Wimmer, and N. M. Tallan	8. CONTRACT OR GRANT NUMBER(s)
9. PERFORMING ORGANIZATION NAME AND ADDRESS: Processing and High Temperature Materials Branch Metals and Ceramics Division, Air Force Materials Laboratory, WPAFB, Ohio	10. PROGRAM ELEMENT, PROJECT, TASK AREA & WORK UNIT NUMBERS: 61102F 70210273
11. CONTROLLING OFFICE NAME AND ADDRESS: Same	12. REPORT DATE: May 1976
	13. NUMBER OF PAGES: 72
14. MONITORING AGENCY NAME & ADDRESS (if different from Controlling Office): I. Bransky, James M. Wimmer, Norman M. Tallan	15. SECURITY CLASS. (of this report): Unclassified
	15a. DECLASSIFICATION/DOWNGRADING SCHEDULE

16. DISTRIBUTION STATEMENT (of this Report)

Approved for public release; distribution unlimited

16 AF-7021 17 7021Q2

17. DISTRIBUTION STATEMENT (of the abstract entered in Block 20, if different from Report)

18. SUPPLEMENTARY NOTES

19. KEY WORDS (Continue on reverse side if necessary and identify by block number)

ceramics
impact resistance
silicon nitride
silicon carbide
sialon
aluminum oxide
dynamic strength

20. ABSTRACT (Continue on reverse side if necessary and identify by block number)

Two mechanisms can lead to failure of ceramics under impact, 1) failure due to flexural stresses, and 2) failure due to Hertzian type cracks introduced locally by the impactor. An instrumented drop-weight test designed to study failure due to flexural stresses is described and used to study various forms of silicon nitride and silicon carbide up to 1300°C. Results on alumina and sialon are included for comparison. From the standpoint of impact resistance hot-pressed silicon nitride is the best material.

DD FORM 1 JAN 73 1473 EDITION OF 1 NOV 65 IS OBSOLETE

SECURITY CLASSIFICATION OF THIS PAGE (When Data Entered)

012320

AE

PREFACE

This report was prepared by the Processing and High-Temperature Materials Branch, Metals and Ceramics Division, Air Force Materials Laboratory, Wright-Patterson Air Force Base, Ohio. The research reported on covered the time period from June 1975 to February 1976 while Dr. I. Bransky was working in the AFML as a Visiting Scientist under Contract F33615-73-C-4155 held by Technology, Inc., Dayton, Ohio. Dr. Bransky is permanately employed by Israel's Ministry of Defense. Dr. J. M. Wimmer (AFML/LLM) was the government Project Scientist. Much of the work was carried out in the AFML Impact Mechanics Laboratory and their outstanding cooperation is gratefully acknowledged. This report was submitted 17 March 1976.

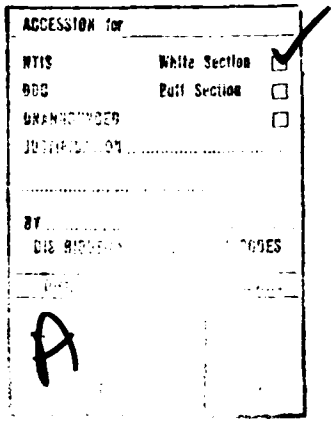

TABLE OF CONTENTS

TABLE OF CONTENTS (continued)

LIST OF ILLUSTRATIONS

LIST OF ILLUSTRATIONS (continued)

LIST OF TABLES

LIST OF TABLES (continued)

SECTION I

INTRODUCTION

Ceramics are currently being considered for use in gas turbine engines in order to increase the turbine inlet temperature to the vicinity of 1370°C (2500°F). In this application the impact resistance of ceramics is of great interest since foreign object damage can be a severe, limiting problem. The impact velocities of primary interest are in the range of 400-1000 f/s. The rotational velocity of the turbine wheel is in the vicinity of 6×10^4 rpm, resulting in a linear, blade tip velocity of about 1000 f/s. This would be the highest effective velocity that a particle carried by the gas stream would impact the rotor blades. Since the velocity of the gas itself is about 400 f/s, this would be the highest effective velocity that particles carried by the gas stream would impact the stator vanes.

The room temperature impact resistance is also of interest since turbine parts are often subjected to impacts during machining and handling. In addition, lower velocity testing is also of interest since certain features of the impact problem can easily be studied at lower velocities.

The object of the present work was to establish the relative impact resistance at both service and room temperature of a number of monolithic ceramics which are candidates for use in turbine engines. Of these, the following ceramics were selected:

Norton,* hot-pressed Si_3N_4, NC-132.

Norton, hot-pressed SiC, NC-203.

Norton, reaction bonded Si_3N_4, NC-350.

Norton, reaction densified SiC, NC-435.

Two other ceramics were also tested for comparison purposes:

Coors,† slip-cast sintered Al_2O_3, AD 998.

Sialon,‡ sintered.

---

*Norton Co., Worcester, Mass.

†Coors Porcelain Co., Golden, Colo.

‡50 m/o Si_3N_4 - 25 m/o Al_2O_3 - 25 m/o AlN, batch 182 fabricated in-house at AFML (LLM)

The process of strength degredation or failure during the impact of load-bearing brittle materials can occur by one of two mechanisms. The first is failure due to the catastrophic propagation of a pre-existing flaw or crack in an area where flexural stresses are developed as a result of the load generated by the impacting particle. The second mechanism arises from the short range stresses generated by the highly localized contact force between the ceramic and the particle. The tensile component of this stress field will cause, at a critical loading, a cone shaped crack known as a Hertzian crack, and will give rise to either strength degradation or complete fracture. In the present work two experiments were designed to study these mechanisms, a drop-weight test (DWT) and a ballistic test. In the DWT a simply supported beam was impacted with a relatively large, low-velocity steel ball (1/2" - 5/8" in diameter). Here, the contact force was much less than the critical level required for Hertzian cracking, and all failures occurred as a result of flexural stresses. In the case of the ballistic tests a square, relatively thick, plate was impacted with a high-velocity steel ball (0.177" in diameter). Here the failure mechanism depended on the method of support. With a ceramic ring supporting the four corners of the plate failure occurred because of flexural stresses, while Hertzian damage could be observed when the plate was fully supported by a massive ceramic rod. This report will discuss the drop-weight tests only; the ballistic tests will be the subject of a second report.

SECTION II

DROP-WEIGHT TEST (DWT)

The impact resistance, in terms of the absorbed energy to fracture, is conventionally obtained for metels using heavy pendulum impact machines in the Charpy or Izod configuration. In the Charpy configuration the sample is clamped at both ends and the energy loss of the pendulum during fracture is considered to be a measure of the impact resistance. This approach works well for metals, where large amounts of energy are absorbed in the failure process. However, ceramics have much lower fracture energies than metals, and the measured pendulum energy loss is predominately due to losses in the impact machine itself. The only really reliable means of obtaining the fracture energy for brittle materials is from instrumented impact tests. Most instrumented impact tests utilize a pendulum type impact machine in the Charpy mode. The tup of the pendulum has a force transducer attached, the output of which is recorded on an oscilloscope. Thus, the load as a function of time is obtained. If at the same time the velocity of the pendulum is recorded, the load-displacement dependence can be derived and the integrated area provides the absorbed energy to fracture.

The application of commercial pendulum type impact machines to ceramics suffers from two disadvantages. First, the heavy pendulum is designed for use with metals and does not approach the low mass, high-velocity impacts that ceramics will see in service. The second, and the main one, is the difficulty of utilizing it for high-temperature impact tests. Only a few high-temperature (uninstrumented) impact tests have been reported. In these tests the sample was either quickly withdrawn from the furnace and impacted by the pendulum, thus, suffering a thermal shock, or the sample temperature was maintained by a torch. These experiments at high-temperature suffer from both the problem of maintaining the sample in an isothermal condition and the errors introduced by the unknown energy losses in the machine itself.

An impact test utilizing a free falling ball, which is better tailored for ceramics, was described by Aquaviva,[1] who used it to compare the notched and unnotched impact resistance of various ceramics for armor applications. In his measurements the height of the ball was increased after each impact by a small increment until fracture occurred. He assumed that when the free falling ball was stopped by the specimen, its kinetic energy was transformed entirely into internal strain energy of the sample, or failure of the specimen when fracture occurred. Under this entire energy transfer assumption, which plainly neglects all extraneous energy sinks, the impact resistance is obtained solely from the height of the falling ball. Two problems arise in interpreting such drop-weight experiments:

1. Although the incremental height method reduces the toss energy, i.e., the kinetic energy of the fractured pieces, there is the possibility of a degradation of the measured strength due to fatigue caused by the repeated impacts.

2. The only measurable quantity in the technique described above is the ball height at fracture. Relating the kinetic energy of the ball at fracture to the fracture energy of the sample suffers from the same criticism as the uninstrumented Charpy test, i.e., unknown energy sinks other then those required to fracture the sample.

The problem of impact fatigue was checked in the present work. It was found that for the number of impacts and impact levels employed in the drop-weight tests, impact fatigue was not observed.

The second problem was eliminated by measuring the actual dynamic stress using a strain gage attached to the tensile side of the impacted sample. This method will be referred to as an instrumented DWT.

The following quantities can be determined from the instrumented DWT at room temperature:

1. The maximum tensile strain on the sample face opposite the impact point

2. The time of strain build-up, and thus the strain rate

3. The elastic modulus of the specimen material, which can be calculated from the free vibration of the sample.

4. Assuming elastic behavior up to fracture, an assumption which is justified for ceramics, the maximum stress can be calculated from Hook's Law. The value thus obtained at fracture is the three point dynamic bend strength of the material at the strain rate determined in (2).

5. From the maximum strain at fracture and the elastic modulus, the elastic energy (EE) stored in the sample can be calculated from elastic beam theory. This energy at fracture is for all practical purposes directly related to the impact resistance of a sample which fails due to a flexural stress.

6. Since the kinetic energy of the ball prior to impact is known and is equal to the potential energy (PE) of the ball at rest, the ratio of energy transfer, EE/PE, can be determined and compared with the assumption of entire energy transfer, EE/PE = 1.

7. Using the experimental energy transfer ratio determined at room temperature, a good approximation for the dynamic strength and impact resistance of a material can be obtained from an uninstrumented DWT at high-temperatures, where strain gages are not applicable.*

---

*Alternatively a laser technique can be used to measure the dynamic beam deflection at high-temperatures[16]. The results show that the use of the room temperature energy transfer ratio at high-temperature is valid.

SECTION III

EXPERIMENTAL PROCEDURES FOR THE INSTRUMENTED DWT AT ROOM TEMPERATURE AND THE UNINSTRUMENTED DWT AT HIGH-TEMPERATURE

1. Room Temperature Measurements

All specimens for both room temperature (RT) and high-temperature (HT) measurements were bars having dimensions 1.73" x 0.25" x 0.125". The specimen was supported at each end by an alumina tube as shown in Fig. 1. A strain gage was cemented to the center of the bar opposite the point of impact. The strain gage used was Micro Measurements CEA-06-062UW with grid resistance R_g = 350.0 $\pm$ 0.3% ohms, gage factor GF = 2.155 $\pm$ 0.5%, and grid dimensions 0.065" x 0.120" (the length of the grid was aligned with the sample length). The strain gage was attached to the specimen by Micro Measurements AE15 cement. A Wheatstone bridge was used to measure the dynamic change of strain gage resistance. The output of the bridge, one arm of which contained the strain gage, was displayed on an osciloscope (Tektronix 556). The strain, ε, was calculated from the osciloscope trace using the relation:

$$\varepsilon = \frac{E \cdot \Delta R_{cal}}{GF \cdot \Delta E_{cal} \cdot R_g} \qquad (1)$$

where E is the dynamic output of the strain gage, ΔR_{cal} is the change of the bridge arm resistance containing the strain gage on connecting a 49.900 ohm resistance in parallel with the strain gage and ΔE_{cal} is the output of the bridge for ΔR_{cal} change. The value of ΔR_{cal} used was 2,438 ohms.

The specimens were impacted by a 1/2" diameter steel ball weighing 8.30g. Some of the high strength specimens were also impacted by a 5/8" diameter steel ball weighing 16.29g. The ball was held by suction in a small inverted cup and was released for free fall by closing a vacuum valve. The cup could be adjusted on a heavy cathetometer stand and could be fixed at any height from 15-120cm above the sample. Carbon paper on a dummy alumina bar was used to mark the impact point, so that the apparatus could

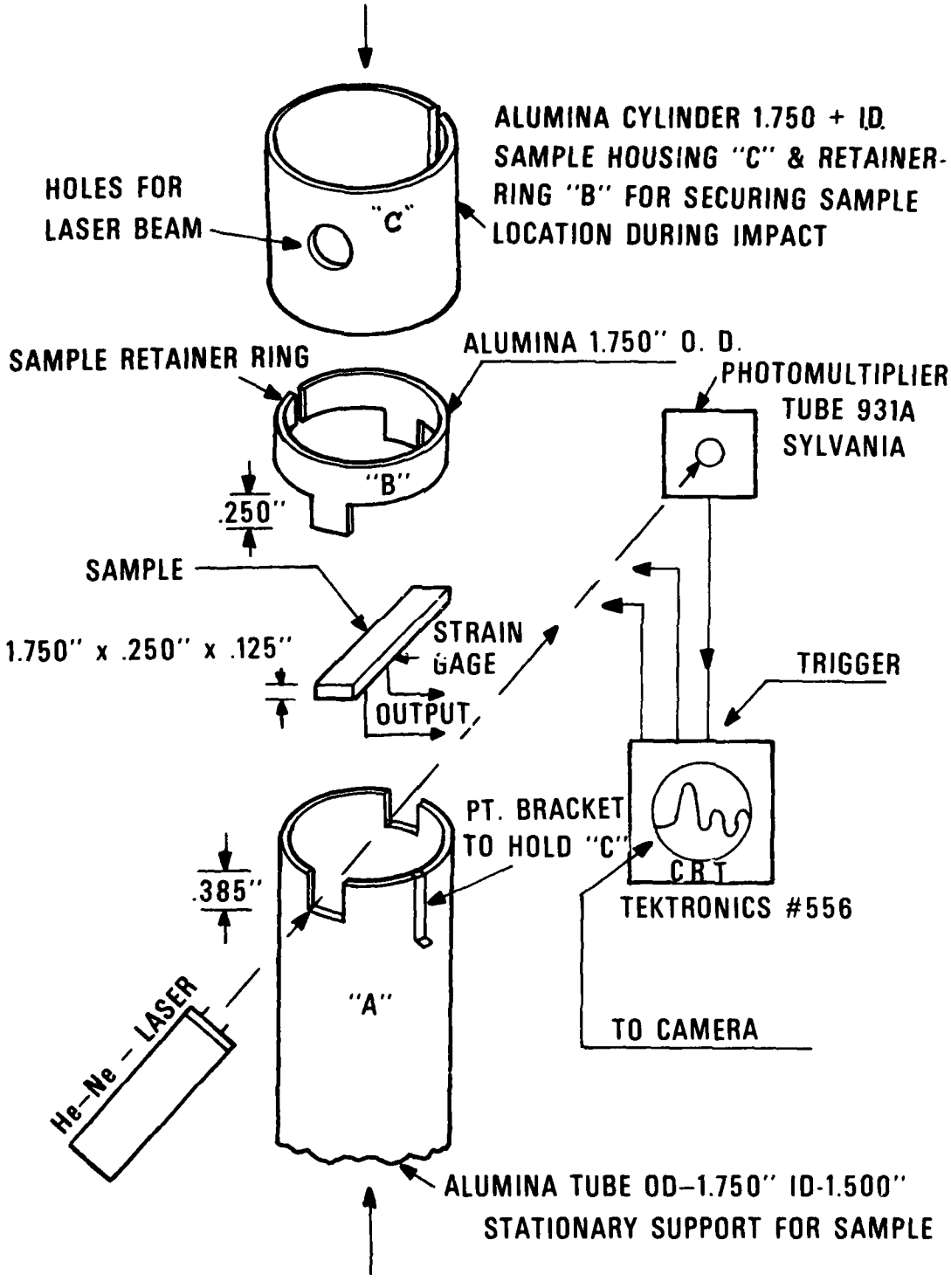

Figure 1. Schematic Diagram of Strain Gage Instrumented DWT Apparatus

be aligned to obtain impact at the specimen center. Center hits were obtained with great accuracy up to the maximum height used. The osciloscope was triggered a few tenths of a millisecond prior to impact by a photo-multiplier pulse signal caused by the ball intersecting a laser beam. The arrangement is shown in Figs. 2-4. The osciloscope trace was photographed at each height, and the height was incrementally increased until fracture occurred.

2. High-Temperature Measurements

The impact resistance was also measured at 1300°C using the same sample holder, but without a strain gage. A vertical alumina tube furnace open on both ends contained the specimen holder and the specimen The furnace has a lid which was removed prior to impact. The specimens were impacted repeatedly with increasing height until fracture occurred. The high-temperature DWT arrangement is shown in Figs. 5 and 6.

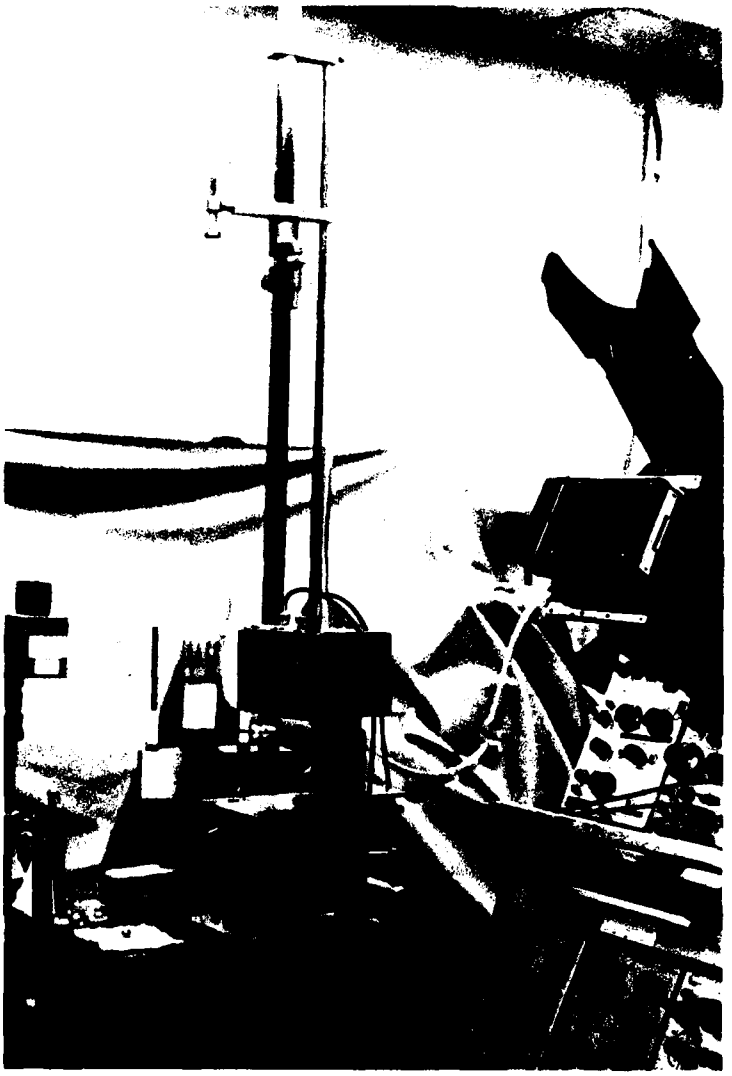

Figure 2. DWT Apparatus; CRT and Camera on Left, Photomultiplier Tube in Center, and He-Ne Laser on Right.

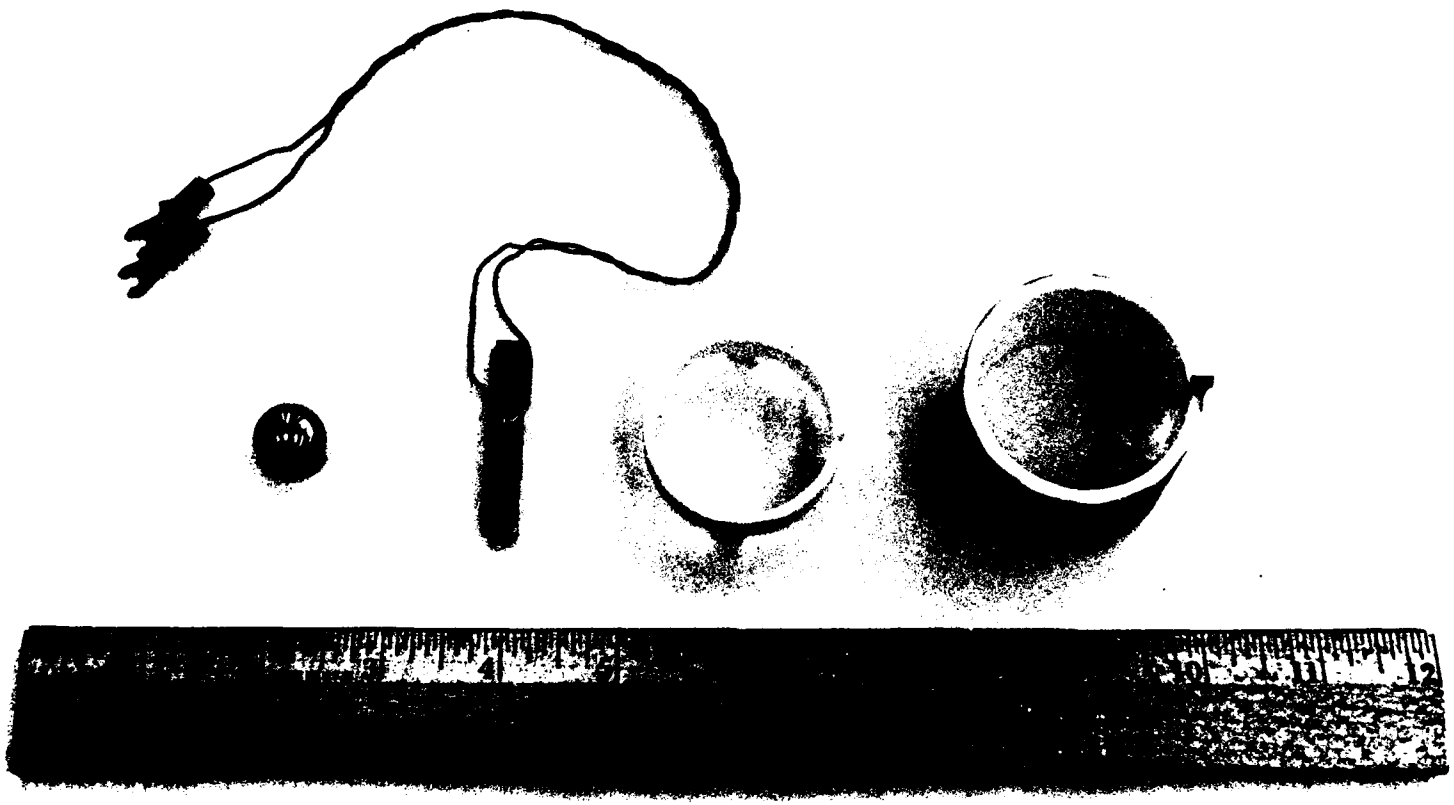

Figure 3. DWT Impactor, Specimen, and Retaining Rings.

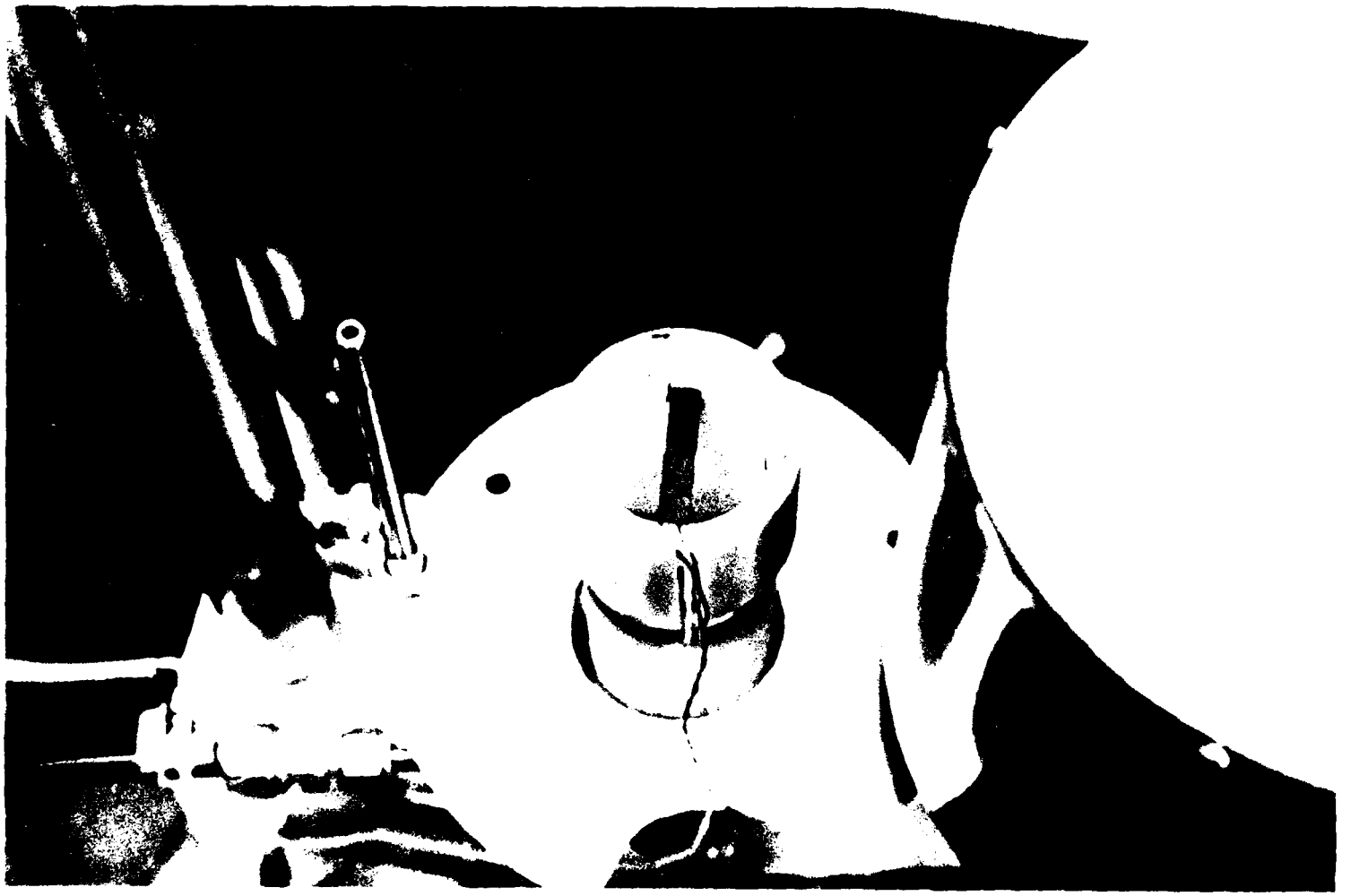

Figure 4. Close-up of Specimen Mounted in DWT Apparatus.

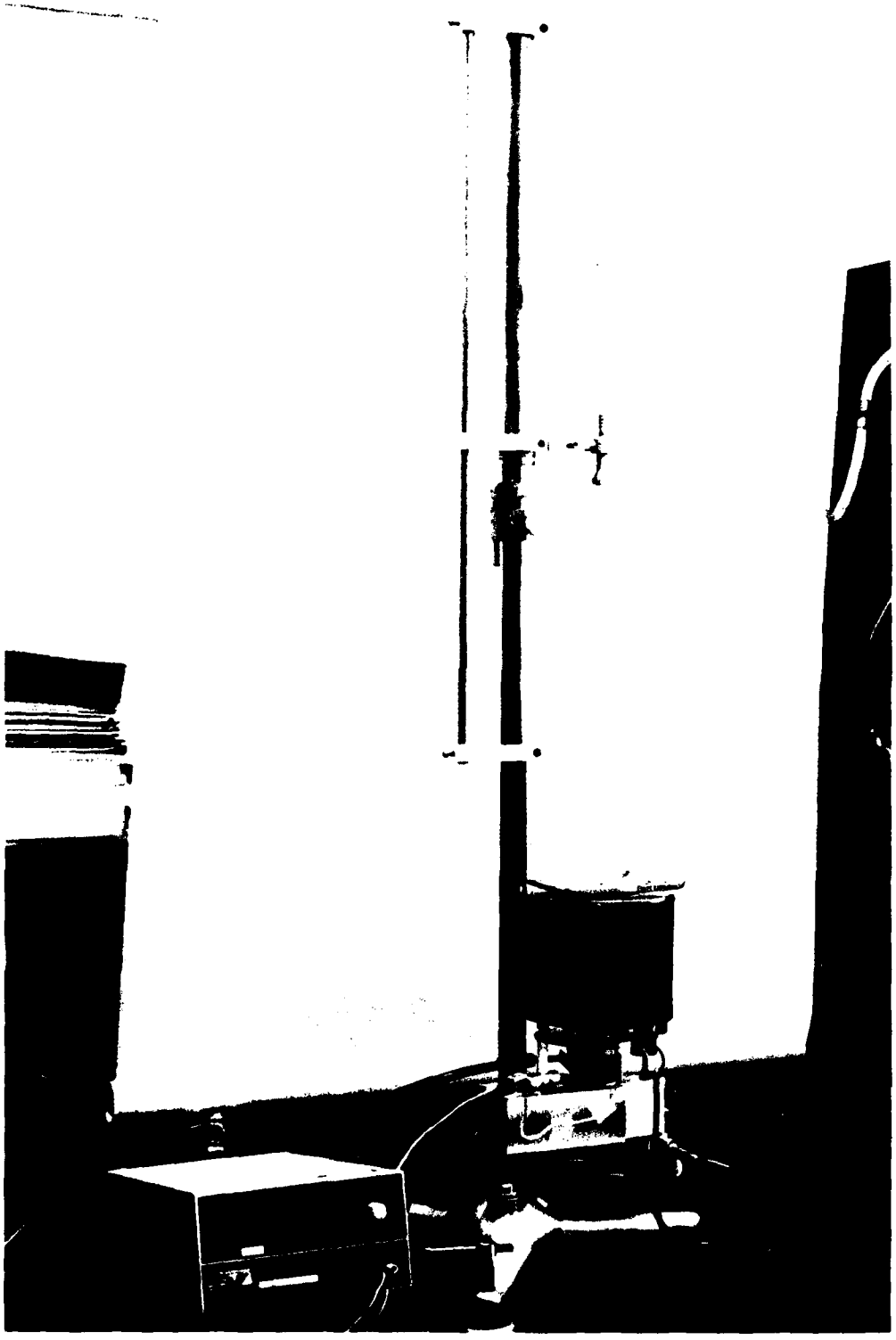

Figure 5. DWT Apparatus for High-Temperature Impact.

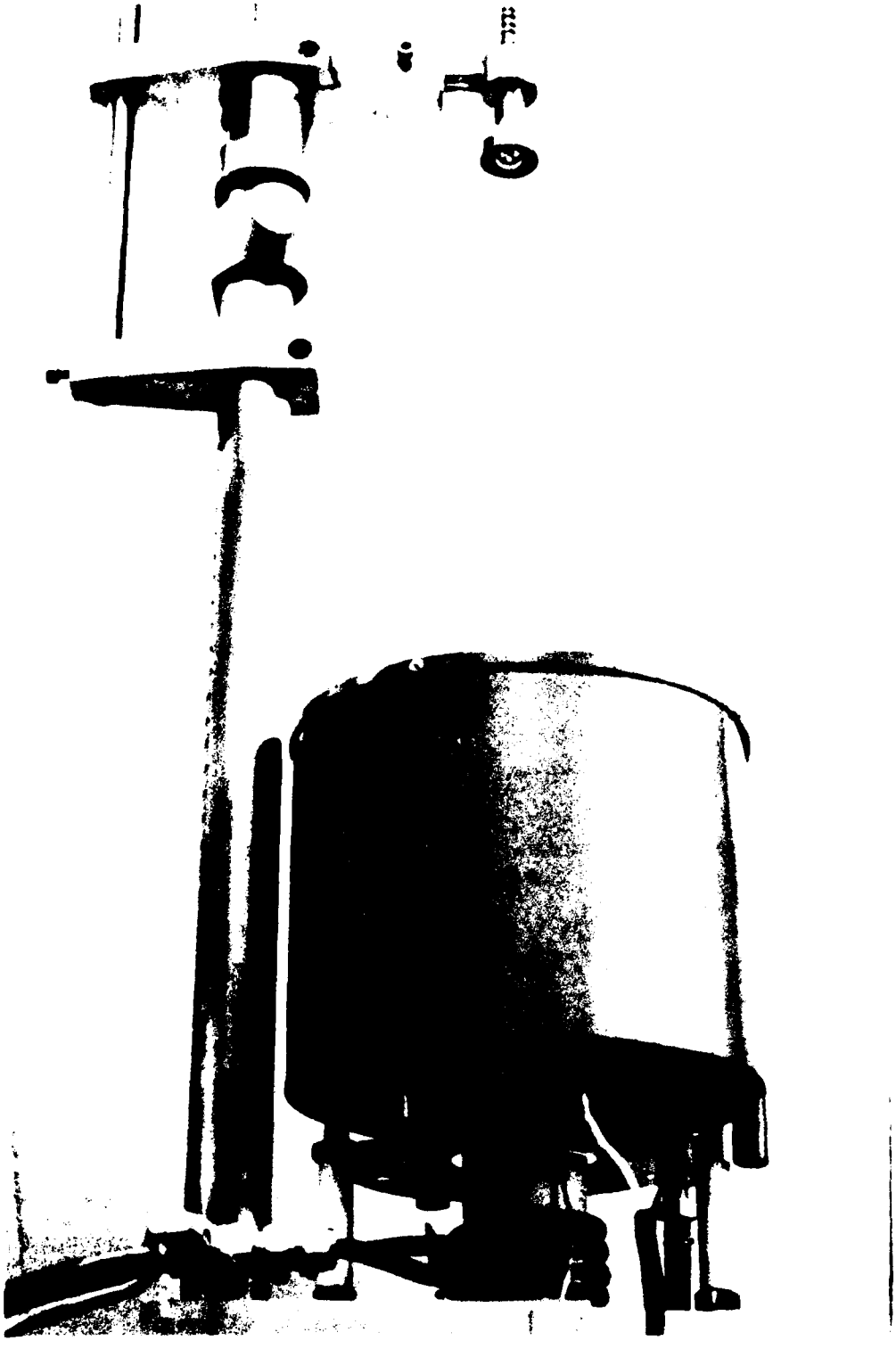

Figure 6. Close-up of DWT Furnace.

SECTION IV

ANALYSIS OF EXPERIMENTAL DATA FOR THE DWT

Before discussing in detail the results of the DWT for each individual ceramic, the method of analyzing the experimental data will be described.

1. *Determination of the Modulus of Elasticity*

A photograph of a typical osciloscope trace is shown in Fig. 7.

The total time of deflection is about 140 ms, after which the speicmen performs free harmonic vibrations. The frequency, f_o, can be accurately determined (in the case of Fig. 7 f_o = 18.39 kHz) and the modulus of elasticity, E, can be calculated from,*

$$E = 0.945 \frac{(f_o)^2 L^4 \rho}{t^2} \tag{2}$$

where: f_o = short transverse frequency (sec^{-1})

L = specimen length (m)

ρ = specimen density (kg/m^3)

E = Modulus (N/m^2)

t = specimen thickness (m)

2. Determination of *Dynamic Bend Strength* From the Instrumented DWT

The object of an instrumented DWT is the determination of the strain on the outer fiber opposite the impact point. The strain, ε, is determined from Eq. 1 and E is determined from Eq. 2. Thus, the dynamic stress is given by:

$$\sigma = \varepsilon E \tag{3}$$

From ε_c, the critical strain at fracture, σ_c, the dynamic 3-pt bend strength can be determined, since Eq. 3 is valid for ceramics up to the point of fracture. Thus, both the elastic modulus and the dynamic strength are obtained on the same specimen from one type of measurement.

---

*Operating Manual for Type FM-500 Magnetest Elastomat, Magnetest Corp., Chicago, IL

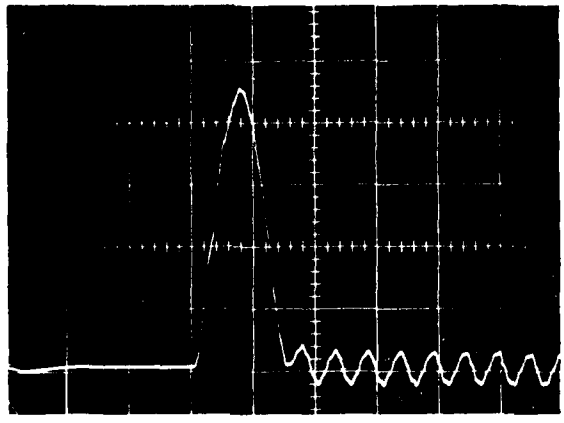

1/2" ball, h = 25 cm

Figure 7. Strain vs. Time for Sub-Critical Impact of AD 998, Al_2O_3, Specimen No. 8 (0.5mV/div, 0.1ms/div)

3. Determination of Dynamic Strength From the Uninstrumented DWT

a. Uninstrumented DWT at Room Temperature

The experimental result of an uninstrumented DWT is the critical height, h_c, at which the specimen fractures for a given ball. To determine the dynamic bend strength, σ_c, from such measurements, one needs a relation between h_c and σ_c. Such a relation can be found in the following manner. From the results of the instrumented DWT it was found that the ratio of elastic energy, EE, in the specimen to the kinetic energy of the ball at impact (equal to the potential energy, PE, of the ball at rest) was constant for all heights including the critical height, h_c, for specimens of the same material impacted by steel balls of the same size. Applying the elastic energy formula for a simple supported beam loaded at the center,* the ratio is:

$$\alpha = \left(\frac{EE}{PE}\right) = \left(\frac{EE}{PE}\right)_c = \frac{(V\sigma^2/18E)}{mgh} = \frac{(V\sigma_c^{\,2}/18E)}{mgh_c} \tag{4}$$

where α is a constant up to the point of fracture. Thus, the room temperature strength of an uninstrumented DWT specimen was obtained from the relation:

$$\sigma_c = \left\{\alpha_{av} \cdot \frac{18Emgh_c}{V}\right\}^{1/2} \tag{5}$$

where m = ball mass, V = sample volume between supports, and α_{av} is the average value of the ratio EE/PE obtained from the instrumented DWT on the same material using an identical ball.

b. Uninstrumented DWT at High-Temperature

The result of a high-temperature DWT is also a critical height, h_c, at which the specimen fractures. To use Eq. 5 for high-temperature experiments, however, the temperature dependence of E and α_{av} should be taken into account.

*The time of loading is sufficiently long for the statically derived beam formulae to be valid.

In order to determine the temperature dependence of α_{av} an instrumented DWT was designed[16] to measure the dynamic deflection at high-temperature. The technique utilizes a laser beam whose intensity changes due to the specimen's deflection into the cross sectional area of the beam upon impact. The change in light intensity is detected by a photomultiplier tube and fast oscilloscope. Deflections of 5 μm are easily detected.

The results at 1300°C for NC-132, Si_3N_4 and NC-203, SiC indicate that α_{av} does not increase by more than a factor of E/E(HT) directly canceling the increase in E with increasing temperature. Thus, Eq. 5 can also be used at high-temperature with the values of E and α_{av} determined at room temperature.

4. Static Strength Measurements

In most cases the DWT specimen broke into two halves which were large enough to use for static, 4-pt bend strength measurements at room temperature. The fixture used had an outer span of 0.75" and an inner span of 0.375". Although the 4-pt static measurements are not exactly comparable to the 3-pt dynamic measurements because of the difference in test technique and sample size, the expected difference in strength is only about 10% if a Wiebull modulus of 10 is assumed.

SECTION V

DROP-WEIGHT TEST RESULTS

1. Coors Al_2O_3 (AD 998)

Specimens were cut and ground to size from 3/16" thick, 5" diameter disks. The specimens were tested in either the as-machined or annealed condition (1 hour at 1300°C in air). In Table I the elastic modulus is given as calculated from the free vibration frequency using Eq. 2. The values thus obtained are compared to the value specified by Coors for this material. T_o is the total time of the beam deflection for a subcritical impact and T_c is the time to fracture for a critical impact. The strain rate at fracture was calculated by taking the ratio of the strain at fracture to the time to fracture (see for example Fig. 8c).

In Table 2 the detailed results of the instrumented DWT on two specimens are given. For each height a photograph of the osciloscope trace was taken; several of these are shown in Fig. 8. The strain at maximum deflection, ε, was calculated from each trace using Eq. 1, which in this case gave a sensitivity of 308.7 μstrain/mV. The maximum tensile stress, σ, opposite the impact point was calculated from Eq. 3 using the measured elastic modulus given in Table 1. The ratio EE/PE was calculated from Eq. 4. The average value of EE/PE for both instrumented DWT specimens was found to be $\alpha_{av} \equiv (EE/PE)_{av} = 0.46$. Therefore, Eq. 5 becomes $\sigma = 5.67 \times 10^8 \sqrt{h}$ (MKS).

In Table 3 the results of the dynamic and static strength measurements are summarized. The strain rates at fracture are indicated along with the point on the specimen at which fracture occurred.

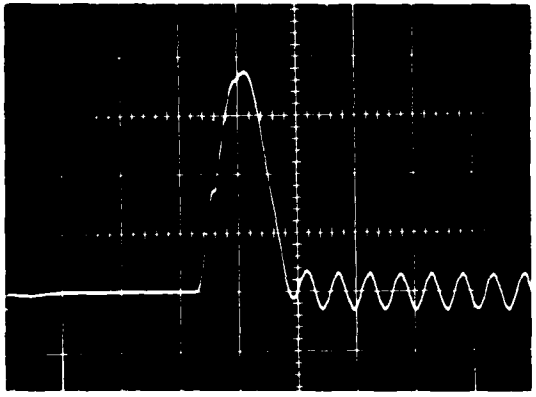

8a. 1/2" ball, h = 20cm

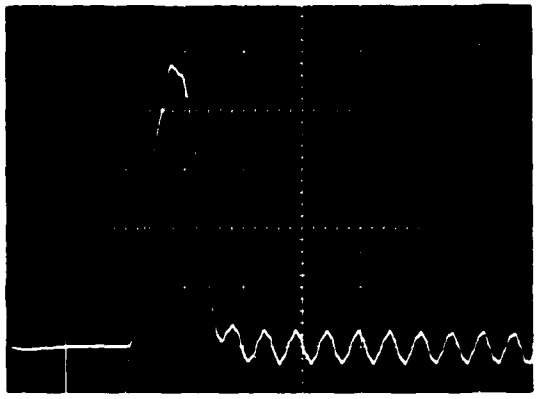

8b. 1/2" ball, h = 30cm

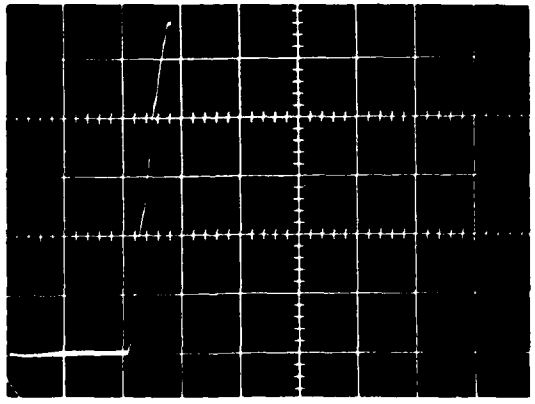

8c. 1/2" ball, h = 43cm

Figure 8. Strain vs. Time for Impact of AD 998, Al_2O_3, Specimen No. 9 (0.5mV/div, 0.1ms/div)

Table 1: Results of Instrumented DWT for AD 998, Al_2O_3

Specimen No.	Specimen Condition	ρ ($\frac{g}{cm^3}$)	E ($\frac{GN}{m^2}$) from Eq.2	E ($\frac{GN}{m^2}$) Coors Value	T_c (μs) Time to Fracture	T_o (ms) Total Time of Deflection	Strain Rate $(sec)^{-1}$
8	As Machined	3.89	401	345	60	140	17
9	" "	3.89	401		60	140	17

Table 2: Detailed Results of Instrumented DWT for AD 998, Al_2O_3

Specimen No.	Figure No.	h(cm)	E(mV)	ε(μ strain)	σ (MN/m^2)	EE/PE
8		15	1.75	538.6	216	0.47
		15	1.70	523.3	210	
		25	2.275	700.2		0.47
	7	25	2.375	731	293	0.51
		35	2.6	800.3	321	
		35	2.7	831	333	0.48
		40	2.9	893	358	
		43	3.15	969.5	389	0.53
		48	3.9	1046.5	420	0.54
9		15	1.53	469.4	188	
	8a	20	1.875	577.1		0.4
		25	2.20	677.1		0.44
		30	2.32	714		0.41
	8b	30	2.375			
		25	2.05	631		0.38
		35	2.65	815.6		0.46
		38	2.70	831		0.47
	8c	43	2.80	861.8	346	0.42

Table 3: Results of Dynamic and Static Strength Measurements for AD 998, Al_2O_3

Specimen No.	Specimen Condition	$\sigma_c(\frac{MN}{m^2})$ Inst. DWT (RT)	$\sigma_c(\frac{MN}{m^2})$ Uninst. DWT (RT)	$\sigma_c(\frac{MN}{m^2})$ Uninst. DWT (HT)	$\sigma_c(\frac{MN}{m^2})^*$ 4-pt Bend Test	Strain Rate $(sec)^{-1}$	Point of Fracture
8	as machined	420				17	center
9	" "	346			364	17	center
1A	annealed		405		280		center
2A	"		387†		280		center
3A	"			387			center

*Measured on pieces of fractured DWT specimen

†Edges were beveled

2. Norton Hot-Pressed Si_3N_4 (NC-132)

Samples were tested either in the as-received or annealed condition (1300°C for 4-hr at 10^{-4} torr). The annealed samples required the use of a 5/8" ball as the fracture did not occur at the maximum height attainable by the DWT tower with a 1/2" ball. In Table 4 , note the increase in the total time of deflection on changing from a 1/2" to 5/8" ball on specimen 24. The detailed results of the instrumented DWT on as-received and annealed specimens are given in Table 5. Note that on the annealed specimens a larger ball was required to fracture the specimen due to the limitation on height. For the 1/2" ball (m = 8.3g) it was found that $\alpha_{av} = 0.615$ and Eq. 5 becomes $\sigma = 5.75 \times 10^8 \sqrt{h}$ (MKS). For the 5/8" ball (m = 16.3g), $\alpha_{av} = 0.71$ and Eq. 5 becomes $\sigma = 8.66 \times 10^8 \sqrt{h}$ (MKS). Note the increase of α_{av} and the total time of deflection with increasing ball mass.

Table 4: Results of Instrumented DWT for NC-132, Si_3N_4

Specimen No.	Specimen Condition	$\rho(\frac{g}{cm^3})$	$E(\frac{GN}{m^2})$ from Eq.2	$E(\frac{GN}{m^2})$ Sonic (2)	T_c (μs) Time to Fracture	T_o (μs) Total Time of Deflection	Drop Weight Ball Dia. (inch)
5	as-received	3.178	313	313	65	140	1/2
24	annealed	3.178	303	313		160	1/2
					100	220	5/8

Table 5: Detailed Results of Instrumented DWT for NC-132, Si_3N_4

Specimen No.	Figure No.	Ball Size	h(cm)	E(mV)	ε(μ strain)	σ MN/m^2	EE/PE
3	9a	1/2"	38	3.65	1167*	365	0.68
		"	43	3.8	1215		
		"	48	3.87	1237	387	0.6
	9b	"	53	4.1	1311		
		"	58	4.45	1423	445	0.66
		"	63	4.8	1534	480	0.66
		"	68	4.9	1564	490	0.68
		"	48	4.0	1279		0.64
	9c	"	70	4.8	1534	480	0.63
24		1/2"	19	2.4	739†	224	0.57
		"	28	2.7	831		0.47
		"	38	3.3	1016	308	0.51
	10a	"	48	3.75	1154	350	0.52
		"	58	4.0	1231	373	0.49
		"	63	4.55	1400	424	0.58
		"	68	4.8	1477	447.5	0.6
		"	73	4.85	1493	452	0.57
		"	78	5.0	1539		0.57
		"	83	5.3	1631		0.6
		"	88	5.7	1754	531.5	0.66
		"	98	5.8	1785		0.61
		"	63	4.8	1477	447.5	0.65
		"	108	5.8	1785		0.55
		"	118	6.35	1954		0.61
		5/8"	35.3	5.1	1570		0.67
		"	43	5.9	1816		0.74
	10b	"	48	6.15	1893		0.72
	10c	7/16"	48	3.1	954		0.53
		5/8"	58	6.7	2062		0.71
	10d	"	73	7.4	2278	690	0.70

*Strain calculated from strain gage sensitivity of 319.7 μ strain/mV

†Strain calculated from strain gage sensitivity of 307.8 μ strain/mV

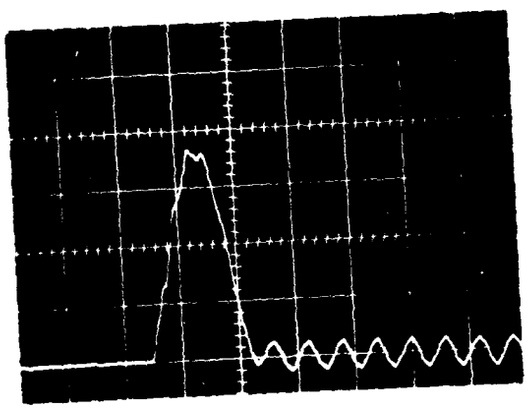

9a. 1/2" ball, h = 38cm

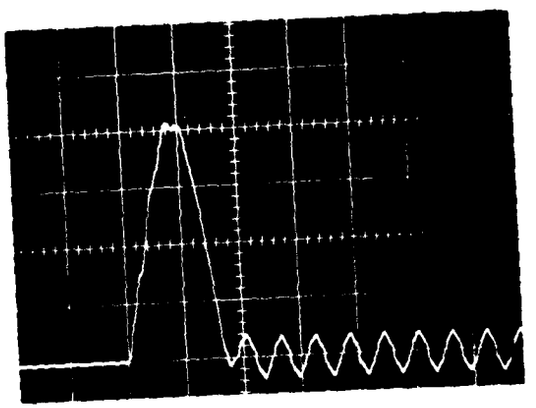

9b. 1/2" ball, h = 53cm

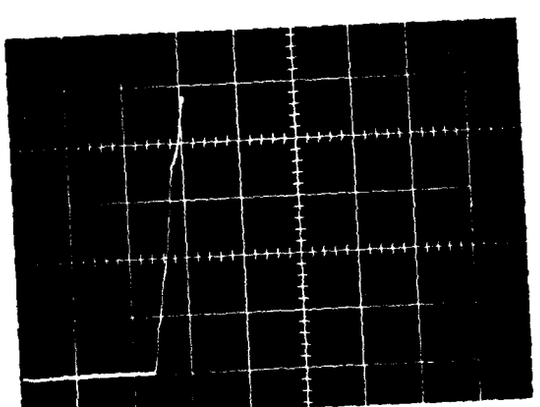

9c. 1/2" ball, h = 70cm

Figure 9. Strain vs. Time for Impact of Si_3N_4, NC-132, Specimen No. 3 (1mV/div, 0.1ms/div)

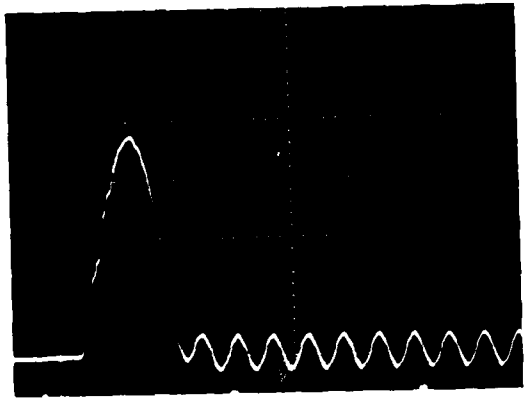

10a. 1/2" ball, h = 48cm, 1mV/div

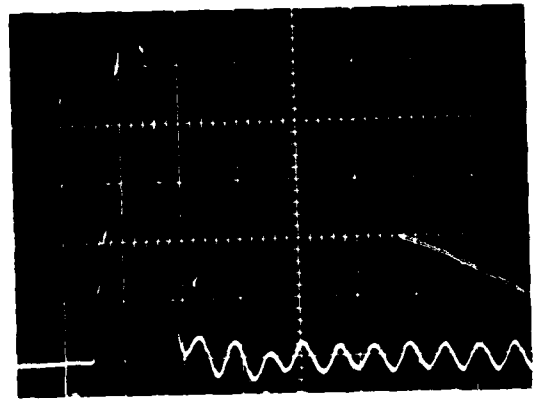

10b. 7/16" ball, h = 48cm, 0.5mV/div

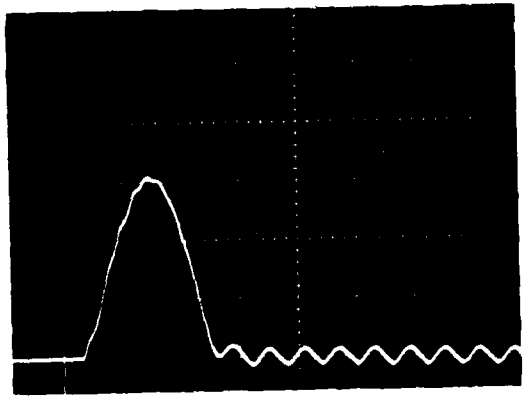

10c. 5/8" ball, h = 48cm, 2mV/div

10d. 5/8" ball, h = 73cm, 2mV/div

Figure 10. Strain vs. Time for Impact of Si_3N_4, NC-132, Specimen No. 24 (0.1ms/div)

Table 6: Results of Dynamic and Static Strength Measurements for NC-132, Si_3N_4

Specimen No.	Specimen Condition	$\sigma_c (\frac{MN}{m^2})$ Inst. DWT (RT)	$\sigma_c (\frac{MN}{m^2})$ Uninst. DWT (RT)	$\sigma_c (\frac{MN}{m^2})$ Uninst. DWT (HT)	$\sigma_c (\frac{MN}{m^2})$ 4-pt Bend Test	Strain Rate $(sec)^{-1}$	Point of Fracture
3	as-received	480				24	center
24	annealed	690				23	center
1 RT	as-received		445				center
2 RT	as-received		540				center
†	annealed				640		
3 HT	as-received			780	811*		center
267	annealed		680				center
268	annealed			794	438*		center
296	as-received				896		

*Measured on pieces of fractured DWT specimens. Both pieces suffered a severe thermal shock upon fracture of the DWT specimen which could be the reason for the low 4-pt bend strength of specimen #268.

†Obtained on a 2"x1/4"x1/8" bars

3. Norton Hot-Pressed SiC (NC-203)

Specimens were tested either in the as-received or annealed condition (1300°C for 1 hour in air). Drop-weights were 1/2" steel balls. The average value of (EE/PE) obtained from Table 8 was $\alpha_{av} = 0.60$ and for this case Eq. 5 becomes $\sigma = 6.74 \times 10^8 \sqrt{h}$ (MKS).

Table 7: Results of Instrumented DWT for NC-203, SiC

Specimen No.	Specimen Condition	$\rho (g/cm^3)$	E (GN/m^2) from Eq.2	E (GN/m^2) Sonic (2)	T_c (μs) Time to Fracture	T_o (μs) Total Time of Deflection	Strain Rate $(sec)^{-1}$
5	as-received	3.29	437	436	60	150	20.5
4	as-received	3.29	437	436	50	140	

Table 8: Detailed Results of Instrumented DWT for NC-203, SiC

Specimen No.	Figure No.	h(cm)	E(mV)	ε(μ strain)*	σ (MN/m^2)	EE/PE
5		33	2.6	831	363	0.56
		33	2.6			
	11a	38	2.9	927	403	0.59
		48	3.22	1029.5	450	
		48	3.23			
	11b	58	3.6	1151	503	0.60
		63	3.8	1215	531	0.61
	11c	67	3.83	1224.5	535	0.59
4		33	2.75	879	384	0.61
		38	2.80	895	385	0.62
		38	2.90	927	405	0.59
		43	3.20	1023		0.64
		43	3.05	975		0.58
		48	3.35	1071		0.62
		53	3.45	1103	482	0.60
		58	3.50			
		58	3.55	1135	496	0.58
		63	3.95	1263		
		63	3.95	1262.8	552	0.60
		65	4.10	1311	575	0.61

*Strain calculated from strain gage sensitivity of 319.7 $\frac{\mu \text{ strain}}{\text{mV}}$

Table 9: Results of Dynamic and Static Strength Measurements for NC-203, SiC

Specimen No.	Specimen Condition	σ_c(MN/m^2) Inst. DWT (RT)	σ_c(MN/m^2) Uninst. DWT (RT)	σ_c(MN/m^2) Uninst. DWT (HT)	σ_c(MN/m^2) 4-pt Bend Test	Strain Rate (sec)$^{-1}$	Point of Fracture
4	as-received	573			260*		3mm to side of center
5	as-received	535			464*	20.5	center
1 RT	" "		491				
2 RT	" "		480		456*		center
3 RT	" "		452		482*		3mm to side of center
4 RT	" "		447		544*		center
Mod	" "				480		
16	" "				400*,492*		
13	" "	350			521*		center
1 HT	" "			491	655*		
2 HT	" "			491	647*		center
5 RT	annealed		527				
3 HT	"			527	754		center

*Measured on fractured DWT specimen

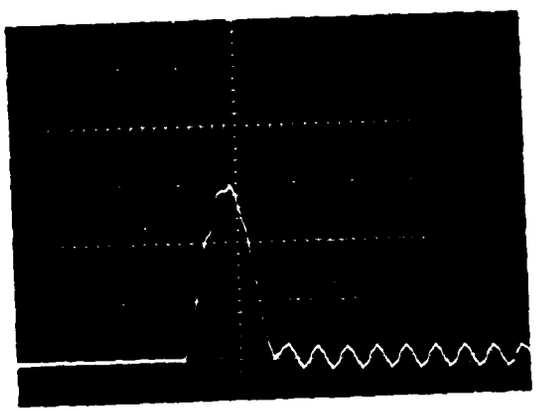

11a. 1/2" ball, h = 38cm

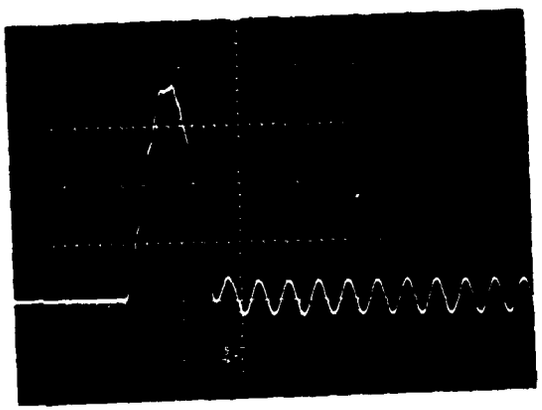

11b. 1/2" ball, h = 58cm

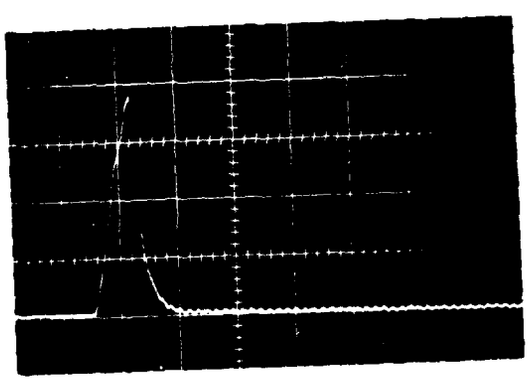

11c. 1/2" ball, h = 67cm

Figure 11. Strain vs. Time for Impact of SiC, NC-203, Specimen No. 5 (1mV/div, 0.1ms/div)

4. Norton Reaction Bonded Si_3N_4 (NC-350)

Specimens were tested in the as-received condition using 1/2" steel balls. The value of $(EE/PE)_{av}$ obtained from Table XI is $\alpha_{av} = 0.86$ and in this case Eq. 5 becomes $\sigma = 5.42 \times 10^8 \sqrt{h}$ (MKS).

Table 10: Results of Instrumented DWT for NC-350, Si_3N_4

Specimen No.	Specimen Condition	$\rho(g/cm^3)$	E (GN/m^2) from Eq.2	E GN/m^2 Sonic (2)	T_c (μs) Time to Fracture	T_o (μs) Total Time of Deflection	Strain Rate $(sec)^{-1}$
10	as-received	2.76	195	172		230	
11	" "	2.76	202		120	225	12.7

Table 11: Detailed Results of Instrumented DWT for NC-350, Si_3N_4

Specimen No.	Figure No.	h(cm)	E(mV)	ε(μ strain)*	σ (MN/m^2)	EE/PE
10		15	3.5	1077	210	0.91
		20	4.05			0.91
		25	4.6			0.94
		15	3.2			0.80
	12	25	4.4			0.85
		30	4.8	1477	290	0.85
11		15	3.45	1062	214.5	0.9
		21	3 92	1207		0.84
		21	3.9	1204		0.8
	13a	28	4.4	1354		0.8
	13b	33	4.95	1523.6	308	0.85

*Calculated from strair gage sensitivity of 207.8 $\frac{\mu \text{ strain}}{mV}$

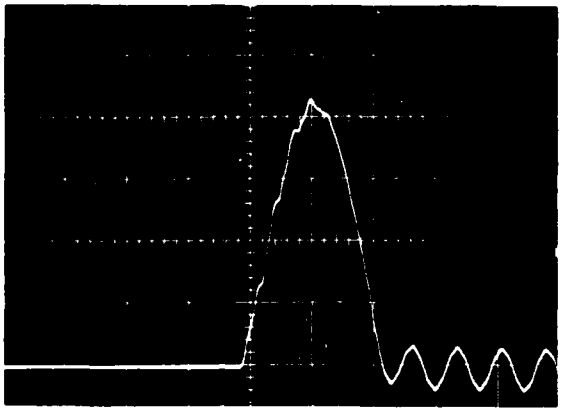

1/2" ball, h = 25cm

1mV/div, 0.1ms/div

Figure 12. Strain vs. Time for Impact of Si_3N_4, NC-350 Specimen No. 10

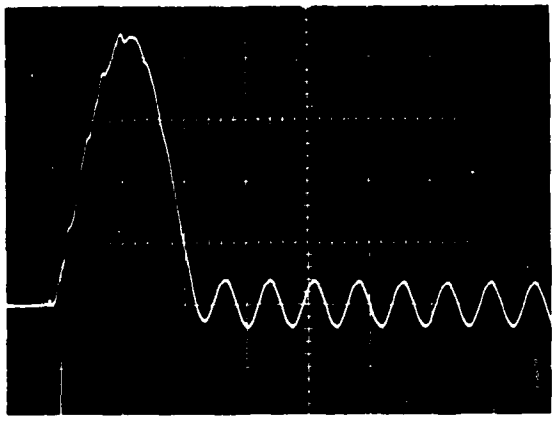

13a. 1/2" ball, h = 28cm

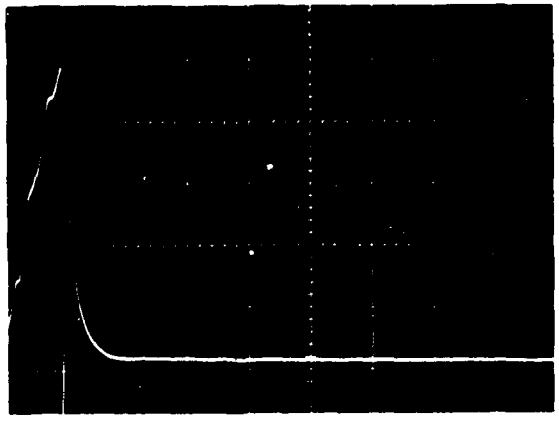

13b. 1/2" ball, h = 33cm

Figure 13. Strain vs. Time for Impact of Si_3N_4, NC-350, Specimen No. 11 (1mV/div, 0.1ms/div)

Table 12: Results of Dynamic and Static Strength Measurements for NC-350, Si_3N_4

Specimen No.	Specimen Condition	$\sigma_c(\frac{MN}{m^2})$ Inst. DWT (RT)	$\sigma_c(\frac{MN}{m^2})$ Uninst. DWT (RT)	$\sigma_c(\frac{MN}{m^2})$ Uninst. DWT (HT)	$\sigma_c(\frac{MN}{m^2})$ 4-pt Bend Test	Strain Rate $(sec)^{-1}$	Point of Fracture
10	as-received	290			221*		3mm to side of center
11	" "	308					
1 RT	" "		316		277*	12.7	5mm to side of center
2 RT	" "		400		306*		chipped on sides
3 RT	" "		343		279*		shattered into many pieces
1 HT	" "			437			"
2 HT	" "			473			"

*Pieces from DWT

5. Norton Reaction Densified SiC (NC-435)

Specimens were tested in the as-received condition using 1/2" steel balls. In general, the specimens of this material exhibited poor behavior. The results were very scattered and appeared to depend mostly on the amount of free Si in the specimens. Note for example, in Figs. 14 and 15 the difference in the free vibration frequency between specimen No. 7 which contained visible free Si and specimen No. 18 in which no Si could be visibly seen. The value of $(EE/PE)_{av}$ obtained from Table 14 was $\alpha_{av} = 0.75$ and thus Eq. 5 becomes $\sigma = 6.43 \times 10^8 \sqrt{h}$ (MKS).

Table 13: Results of Instrumented DWT for NC-435, SiC

Specimen No.	Specimen Condition	$\rho(g/cm^3)$	E (GN/m^2) from Eq.2	E (GN/m^2) Sonic (2)	T_c (μs) Time to Fracture	T_o (μs) Total Time of Deflection	Strain Rate $(sec)^{-1}$
7	as-received	3.03	293		100	220	8.6
18	" "	3.03	342	345	100	160	7.

Note that specimen #7 containing visible free Si has a lower elastic modulus than specimen #18 which showed no visible free Si.

Table 14: Detailed Results of Instrumented DWT for NC-435, SiC

Specimen No.	Figure No.	h(cm)	E(mV)	ε(μ strain)	σ (MN/m^2)	EE/PE
7	14	18	2.7	863	253	0.73
		18	2.6	Fractured		
18	15	13	2.2	703.3	241	0.78
		18	2.1	Fractured		

Table 15: Results of Dynamic and Static Strength Measurements for NC-435, SiC

Specimen No.	Specimen Condition	$\sigma_{c_m}(\frac{MN}{2})$ Inst. DWT (RT)	$\sigma_{c_m}(\frac{MN}{2})$ Uninst. DWT (RT)	$\sigma_{c_m}(\frac{MN}{2})$ Uninst. DWT (HT)	$\sigma_{c_m}(\frac{MN}{2})$ 4-pt Bend Test	Strain Rate $(sec)^{-1}$	Point of Fracture
7	as-received	293				8.6	3 pieces
18	" "	342				7.	3mm to side
1 RT	" "		<200		177*		3 pieces
2 RT	" "		431		295*		
3 RT	" "		363		569*		center
4 RT	" "		306				center
5 RT	" "		406		444*		center
1 HT	" "			421	547*		center
2 HT	" "			<250	131*		5mm to side
1B	" "				32		

*Pieces from DWT

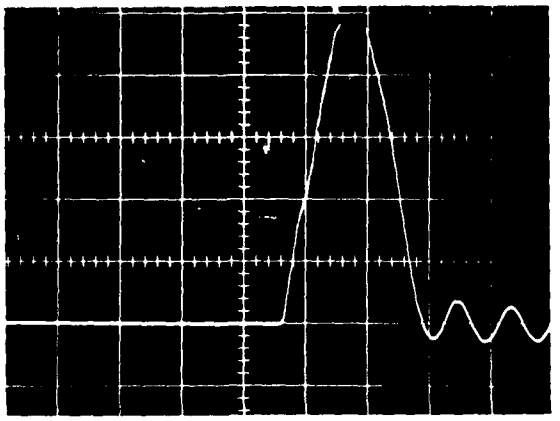

1/2" ball, h = 18cm

0.5mV/div, 0.1ms/div

Figure 14. Strain vs. Time for Impact of SiC, NC-435, Specimen No. 7

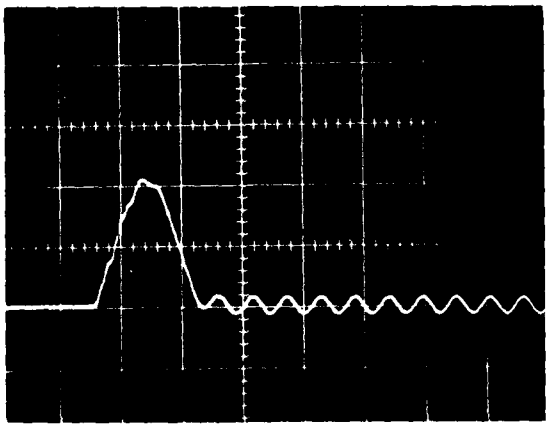

1/2" ball, h = 13cm

1mV/div, 0.1ms/div

Figure 15. Strain vs. Time for Impact of SiC, NC-435, Specimen No. 18

6. Sialon

Sintered specimens of β-sialon having the composition 50 m/o Si_3N_4 - 25 m/o Al_2O_3 - 25 m/o AlN were tested in either the as-machined or annealed condition (1300°C for 1 hour in air). The value of $(EE/PE)_{av}$ obtained from the data of Table 17 was $\alpha_{av} = 0.7$ and Eq. 5 thus becomes $\sigma = 5.61 \times 10^8 \sqrt{h}$ (MKS) for impact with a 1/2" steel ball.

Table 16: Results of Instrumented DWT for Sialon

Specimen No.	Specimen Condition	ρ(g/cm^3)	E (GN/m^2) from Eq.2	T_c (μs) Time to Fracture	T_o (μs) Total Time of Deflection	Strain Rate (sec)$^{-1}$
21	as-machined	3.04	263	75	200	19
22	" "	3.01	256	60	200	26

Table 17: Detailed Results of Instrumented DWT for Sialon

Specimen No.	Figure No.	h(cm)	E(mV)	ε(μ strain)*	σ (MN/m^2)	EE/PE
21		13	2.5	770		0.71
		18	2.95	908	239	0.71
		20	3.0	923	243	0.67
		28	3.7	1139		0.72
	16a	38	4.2	1293	340	0.69
		43	4.5	1385		0.70
	16b†	48	4.72	1453	382	0.70
	16c	58	4.6	1416		
22		18	2.95	908	232	0.71
		28	3.6	1108		0.68
	17	38	4.2	1293		0.69
		44	5.0	1539	394	0.73

*Calculated from strain gage sensitivity of 307.8 $\frac{\mu \text{ strain}}{\text{mV}}$

†At this point the edge of the specimen chipped, note the effect on the free vibration wave form.

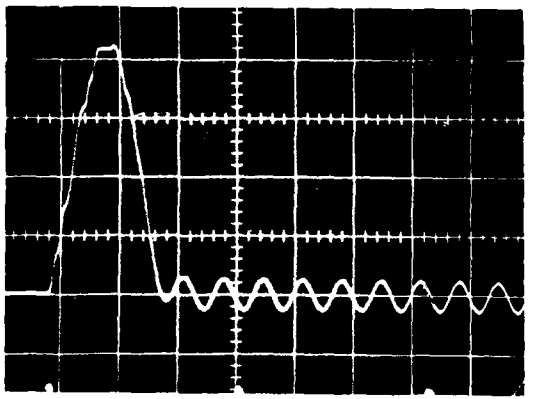

16a. 1/2" ball, h = 38cm

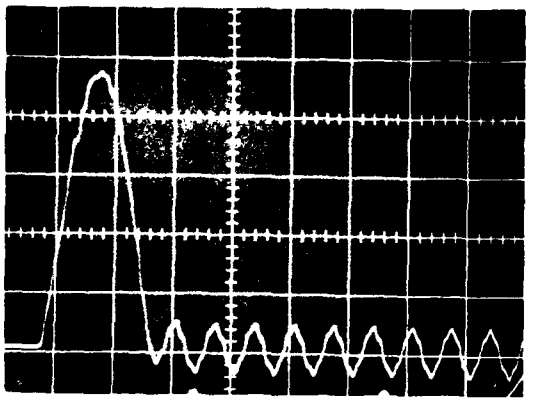

16b. 1/2" ball, h = 48cm

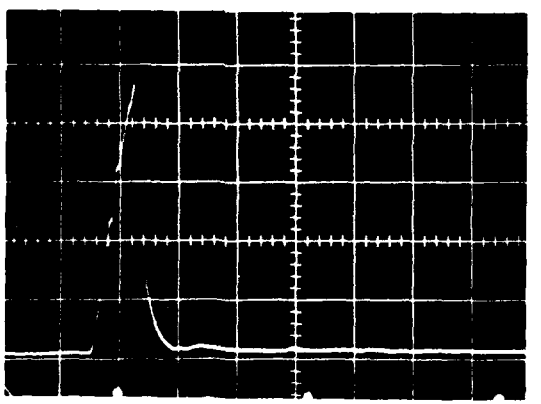

16c. 1/2" ball, h = 58cm

Figure 16. Strain vs. Time for Impact of Sialon, Specimen No. 21 (1mV/div, 0.1ms/div)

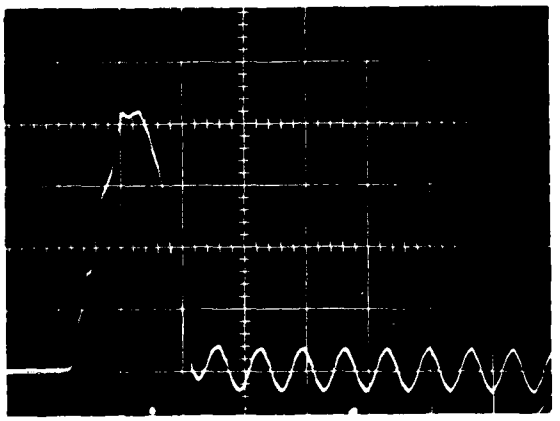

1/2" ball, h = 38cm

1mV/div, 0.1ms/div

Figure 17. Strain vs. Time for Impact of Sialon, Specimen No. 22

Table 18: Results of Dynamic and Static Strength Measurements for Sialon

Specimen No.	Specimen Condition	$\sigma_c(\frac{MN}{m^2})$ Inst. DWT (RT)	$\sigma_c(\frac{MN}{m^2})$ Uninst. DWT (RT)	$\sigma_c(\frac{MN}{m^2})$ Uninst. DWT (HT)	$\sigma_c(\frac{MN}{m^2})$ 4-pt Bend Test	Strain Rate $(sec)^{-1}$	Point of Fracture
21	as-received	382				19	3 pieces
22	" "	394				26	4 pieces
269	" "			490	390*		to side of center
270	annealed		374		251		center

*A piece of DWT at 1300°C, air quenched from 1300°C.

SECTION VI

FRACTOGRAPHY

The fracture surfaces of specimens impacted in the DWT have been examined by use of the scanning electron microscope.

1. Hot-Pressed Si_3N_4 (NC-132)

The fracture surfaces of two as-received specimens impacted at room temperature, two specimens impacted at 1300°C, and one annealed specimen impacted at room temperature were examined. In all five specimens the fracture originated at an edge on the tensile side of the specimen (the side opposite the point of impact). This behavior is illustrated in Fig. 18(a). The fracture appeared to be predominately intergranular both at room temperature, Fig. 18(b), and at 1300°C, Fig. 18(c). Although there is a distinct difference in appearance between the fracture surfaces at room temperature (Fig. 18(b)) and at 1300°C (Fig. 18(c)), all of the sharp corners and edges evident at room temperature being rounded off at high-temperature, it is generally accepted[2] that the fracture is intergranular. Therefore, the difference in appearance might be due to oxidation at high-temperature, although the fractured specimens drop out of the furnace immediately after impact and the exposure of the fracture surface at high-temperature is very short.

2. Hot-Pressed SiC (NC-203)

The fracture surfaces of two room temperature and two high-temperature (1300°C) impact specimens were examined. In contrast to Si_3N_4 NC-132 where fracture always originated at an edge, the fracture origins in NC-203 SiC were not obvious. An example of the fracture surface is shown in Fig. 19(a). Both the room temperature, Fig. 19(b), and the high-temperature, Fig. 19(c), fracture surfaces appeared to exhibit regions of transgranular and intergranular fracture.

(a)

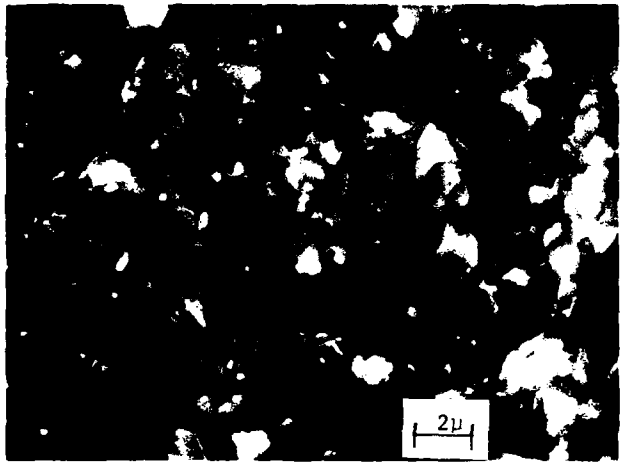

(b)

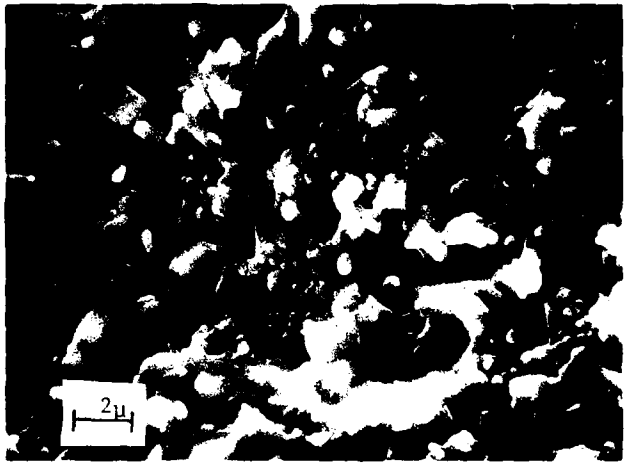

(c)

Figure 18. Fracture Surface of Si_3N_4, NC-132.

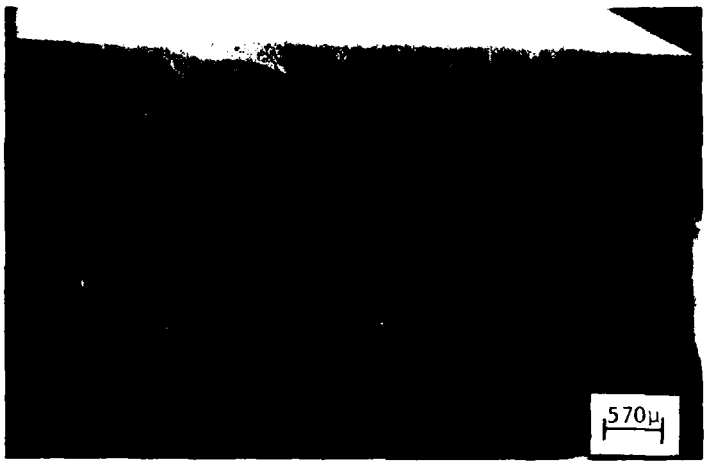

(a)

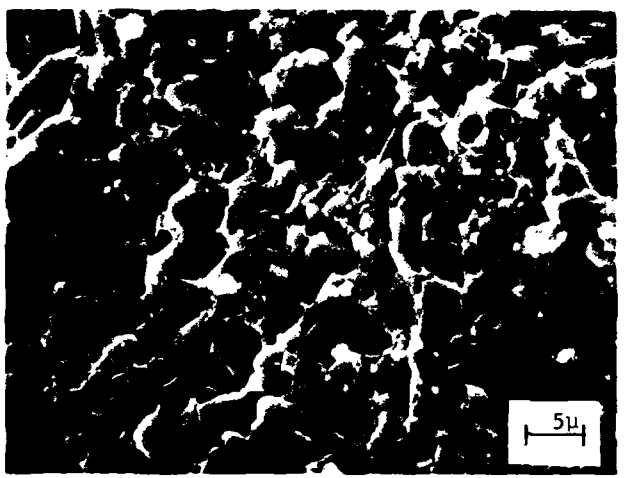

(b)

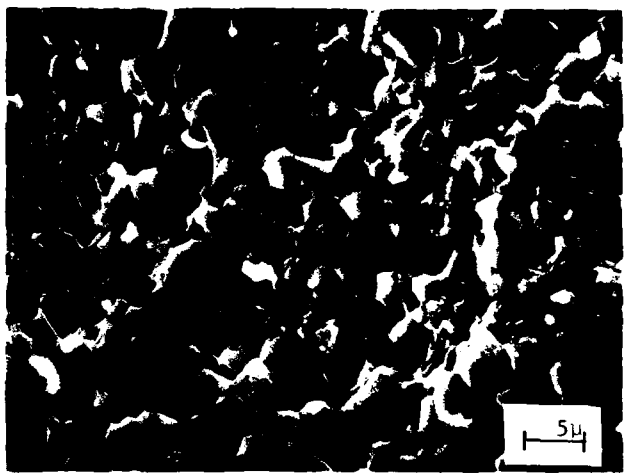

(c)

Figure 19. Fracture Surface of SiC, NC-203.

3. Reaction Bonded Si_3N_4 (NC-350)

One room temperature and one high-temperature (1300°C) fracture surface were examined. In both cases the fracture originated at a pocket of porosity close to the tensile side of the impacted specimen. Figures, 20(a), (b), (c), and (d) illustrate the appearance of the fracture surface and a close-up of the flaw which caused failure. The extent of the flaw on the fracture surface was about 50 μm at room temperature and about 25 μm at 1300°C. The fracture appeared to be predominately intergranular.

4. Sialon

Both a room temperature and a high-temperature fracture surface were examined. In both cases the fracture appeared to initiate at an edge as shown in Fig. 21(a). The fracture appears to be predominately intergranular at both room temperature Fig. 21(b), and at 1300°C, Fig. 21(c).

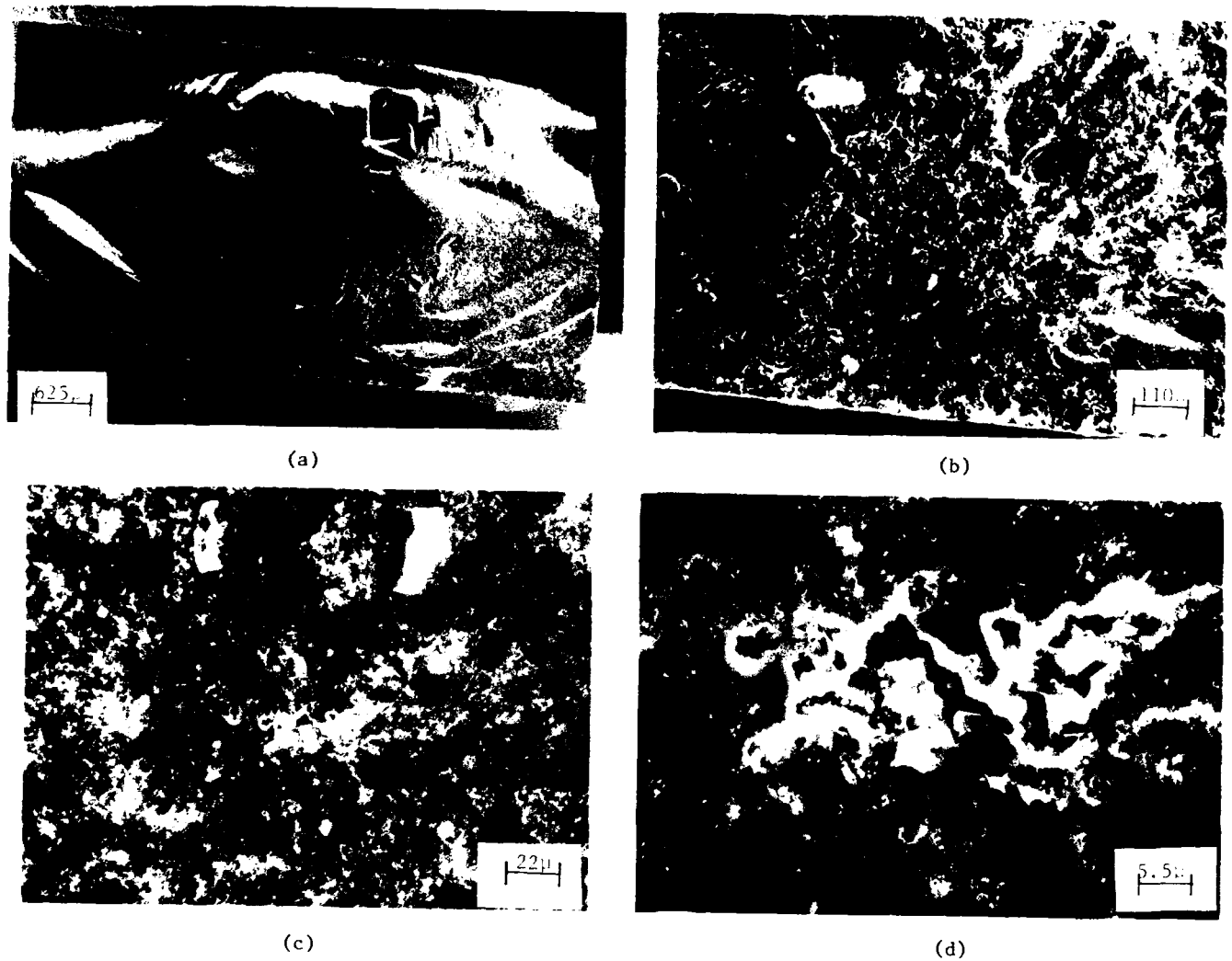

Figure 20. Fracture Surface of Si_3N_4, NC-350.

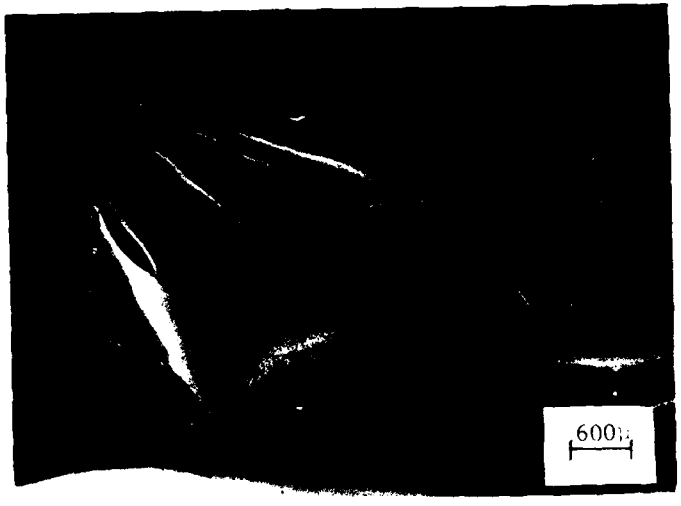

(a)

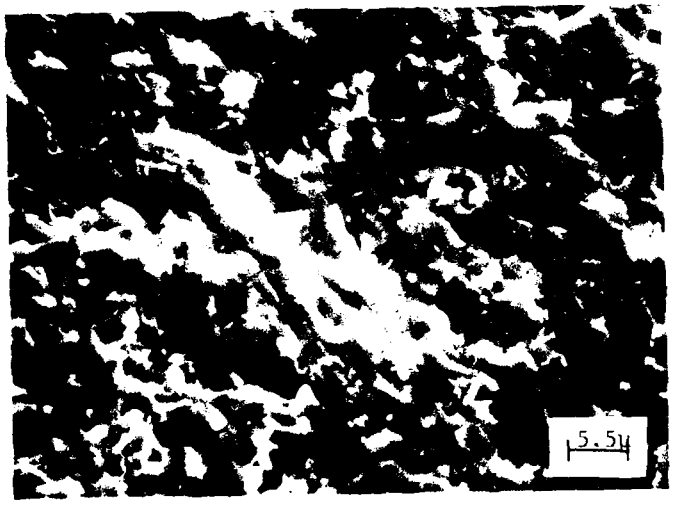

(b)

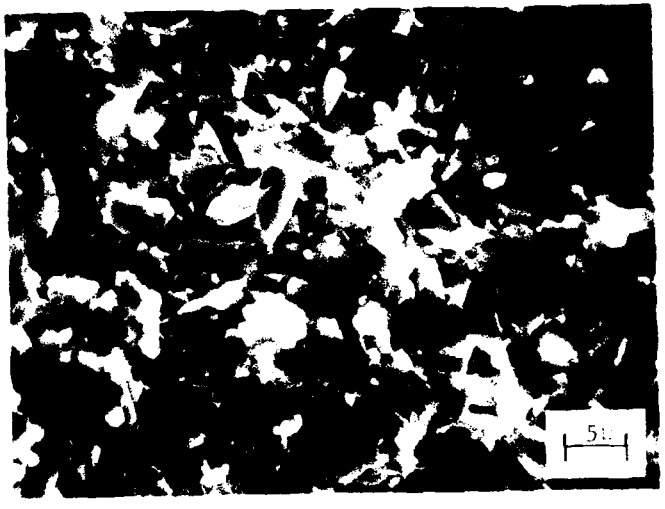

(c)

Figure 21. Fracture Surface of Sialon.

SECTION VII

INSTRUMENTED DWT ON NC-203, SiC CONTAINING A CONTROLLED FLAW

1. Introduction

The method of determining the critical stress intensity factor, K_{IC}, by introducing a single controlled flaw into the tensile surface of a conventional 4-point bend specimen has been used on hot-pressed HS-130[3] Si_3N_4 and hot-pressed NC-203[4] SiC. The surface flaw is produced by a Knoop microhardness indenter. This flaw is "controlled" i.e., its basic shape is relatively constant and its dimensions are a function of the load on the indenter. Such a flaw introduced into the tensile surface determines the strength of the specimen since it is the worst flaw present in the distribution of flaw sizes and orientations.

This well established technique was selected to check the reproducibility of the instrumented DWT, since the dependence of the strength of the ceramic specimen on flaw distribution is eliminated by this method and a constant strength should be obtained on all flawed specimens.

2. Experimental Procedure

Hot-pressed NC-203 SiC samples were used for this study. The controlled flaw was introduced using a Knoop microhardness indenter with a load of 2600 g. The flaw was introduced in the center of the sample with its long diagonal perpendicular to the sample length. A strain gage was applied at the sample center over the flaw by the procedure described previously.

Two specimens were tested in the as-indented condition. Two other specimens were tested after the indented surface was ground to remove a layer of material about 0.025mm thick. Since this thickness is several times the indentation depth, any deformed material associated with the indentation is removed. The remaining surface crack of the last two samples should then be free of the indenter-induced residual stress which would otherwise give rise to a decrease in strength[3]. All samples fractured through the flaw into two pieces.

3. Results

Table 19: Results of Instrumented DWT for NC-203, SiC Containing a Controlled Flaw

Specimen No.	Specimen Condition	σ_c (MN/m^2)	E (GN/m^2) from Eq.2	T_c (μs) Time to Fracture	T_o (μs) Total Time of Deflection	Strain Rate $(sec)^{-1}$
12	as-indented	250	437	55	140	10
17	" "	250	437	55	140	10
14	ground	290	438	60	140	11
15	"	310	437	60	140	12

Table 20: Detailed Results of Instrumented DWT for NC-203, SiC Containing a Controlled Flaw

Specimen No.	h(cm)	E(mV)	ε(μ strain)*	σ (MN/m^2)	EE/PE
12	15	1.75	537		0.51
	17	1.85	569.4	250	0.51
17	16	1.85	569.4	250	0.52
14	18	2.1	646.4		0.6
	21	2.15	661.7	290	0.52
15	13	1.7	523.3		0.54
	18	2.0	615.6		0.54
	23	2.3	707.9	310	0.56

*Strain was calculated from a strain gage sensitivity of 307.8 $\frac{\mu \text{ strain}}{mV}$

SECTION VIII

RELATION BETWEEN DYNAMIC STRESS AND IMPACTOR ENERGY AND MOMENTUM IN A DWT

Two aspects of the impact problem can be considered separately. The first is the relation of the energy and momentum of the impactor to the impulsive loading of the material, while the second is the response of the material to the impulsive loading. Although this report concentrates on the latter the first aspect is treated in this section and the following sections treat the material response aspect.

The treatment of the problem of a ball impacting a simply supported beam is discussed by Goldsmith.[5] The problem is complex and numerical techniques are required for its solution. For practical purposes two approximate approaches can be considered:

1. Energy transfer approach.
2. Contact force approach.

In the first approach it might initially be assumed that at maximum deflection of the specimen the ball is at rest, and that all of its energy has been transferred to elastic energy in the beam. However, this has been found to be incorrect because the ball rebounds before the beam reaches its maximum deflection. Therefore, a better assumption is that a constant portion of the ball energy, PE, is transferred to elastic energy, EE, in the beam at maximum deflection in a DWT, i.e., $EE = \alpha PE$. As shown above, the ratio EE/PE was found to be fairly constant for specimens of the same material impacted by balls of the same size. The average ratios for the materials studied are summarized in Table [21] for a 1/2" ball.

Table 21: Summary of $(EE/PE)_{av}$ for 1/2 Inch Ball

Material	Al_2O_3 AD 998	SiC NC-203	Si_3N_4 NC-132	Sialon	SiC NC-435	Si_3N_4 NC-350
$\alpha_{av} \equiv (EE/PE)_{av}$	0.46	0.60	0.615	0.70	0.75	0.86
E (GN/m^2)	400	437	310	260	340	200

As indicated by this table, the assumption of entire energy transfer made by Aquaviva,[1] i.e., $\alpha = 1$, is only a rough approximation and the estimate of the dynamic strength from Eq. 5 based on this assumption results in values 10-40 percent greater than the actual strength. It appears from Table 21 that for ceramics like sialon and NC-350 Si_3N_4 having low elastic modulus, the entire energy transfer approximation is fairly good.

In the second approach a relation which describes the contact force exerted by the impactor on the beam is required. One such relation that has been proposed[9] is derived[5,6] from the Hertz Law of contact and gives the maximum compressive force, P_{max}, acting between a sphere and a massive plane surface. This force is given by,[6]

$$P_{max} = 1.14 \left\{[16/(9\pi^2)][m^3 v^6 R]/(k_1 + k_2)^2\right\}^{1/5} \qquad (6)$$

where, $k_1 = (1-\nu_1^2)/(\pi E_1)$, $k_2 = (1-\nu_2^2)/(\pi E_2)$

ν = Poisson's ratio, and the subscripts 1 and 2 refer to the ball and plate respectively. If Eq. 6 is applied to the DWT, then the maximum load exerted on the beam by an impacting ball can be related to the maximum outer fiber tensile stress by employing the relation between load and stress for a simply supported beam.

$$\sigma_{max} = \frac{3P_{max}\ell}{2t^2 w} \qquad (7)$$

where t = beam thickness, w = beam width and ℓ = length between beam supports.

For the conditions of the DWT used in this study Eqs. 6 and 7 predicted a stress about a factor of three larger than the measured value. This is evidently due to flexure of the beam during impact, (cf. Ref. 4, pp. 111). In fact, the force calculated from Eq. 6 will always be larger than the actual value if the impacted object can deflect during the impact duration.

Although the energy transfer approach requires the introduction of the parameter α, and Eq. 6 does not give the correct magnitude of the contact force, the data were nevertheless used to determine the dependence of the stress on the ball velocity and radius for comparison with the predictions of these approaches. In Figs. 22a and b, log ε is plotted vs. log (2R) for constant height for data obtained on NC-203 SiC and NC-132 Si_3N_4 using balls from 1/4" to 5/8" in diameter. ε is the strain gage output which is directly proportional to the stress. From these plots it is found that σ_{max} is proportional to R^2. Also, log h was plotted vs. log ε, Fig. 23, for constant R for six different ceramics. The slope of the lines was calculated by the method of least squares with the result that $\sigma_{max} \propto h^{1/n}$

where, $1.6 \leq n \leq 2$ (average n = 1.78).

From the energy transfer approach and Eq. 5 the dependence of the stress on ball height and radius is expected to be $\sigma \propto \alpha R^{3/2} h^{1/2}$ where $v = \sqrt{2gh}$ has been used (g = gravitational constant). This dependence agrees with the experimental data if α is dependent on $R^{1/2}$, which is supported by the data in Table 5 for NC-132 Si_3N_4. Since the ball mass is $m = (4/3)\pi R^3 \rho$, Eq. 6 predicts a stress dependence of $\sigma \propto R^2 h^{3/5}$ for the contact force approach. Again, this dependence is consistent with that observed in Figs. 22 and 23.

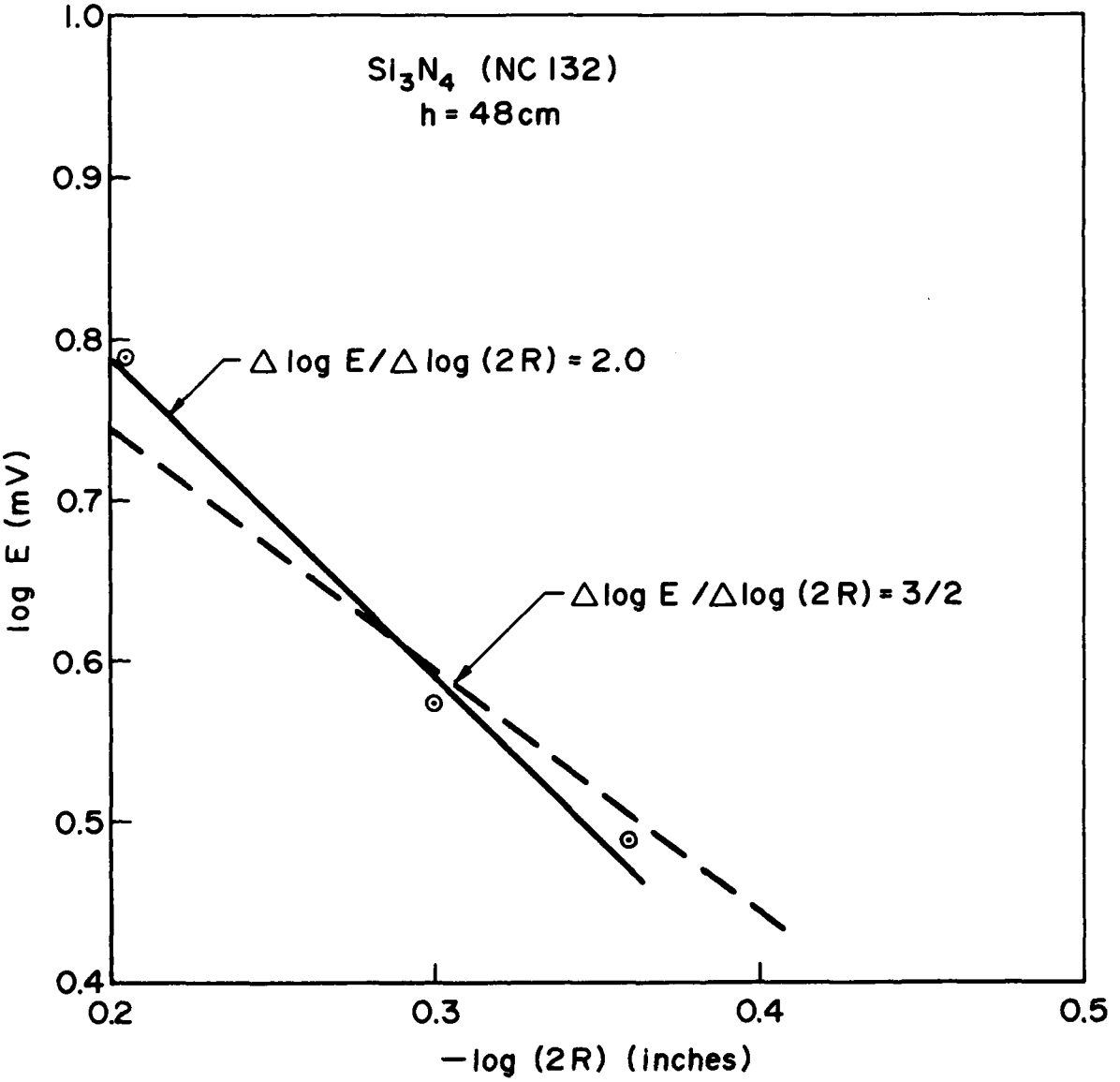

Figure 22a. Dependence of Dynamic Stress at Maximum Deflection on Ball Size Si_3N_4 (NC-132).

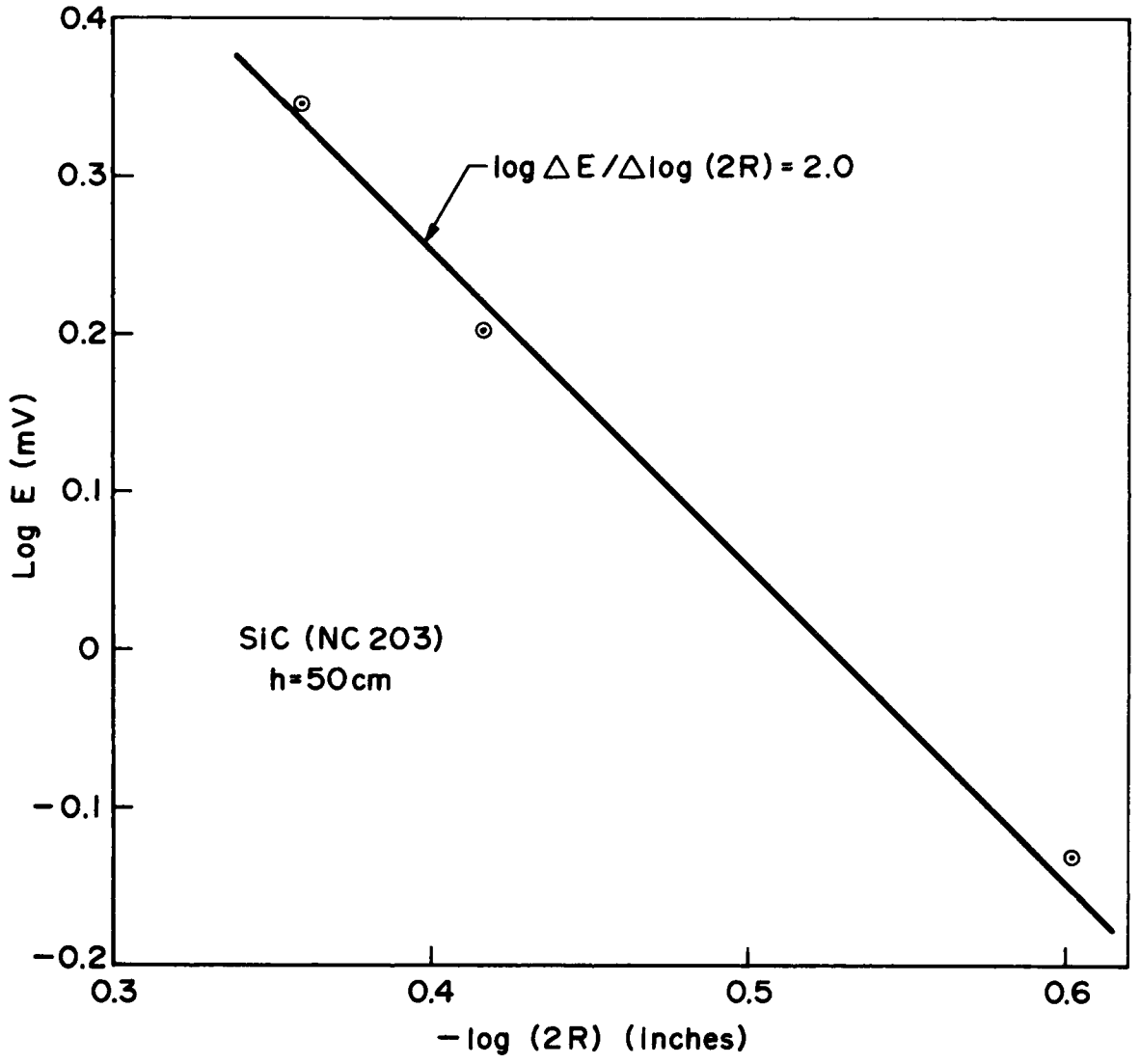

Figure 22b. Dependence of Dynamic Stress at Maximum Deflection on Ball Size SiC (NC-203).

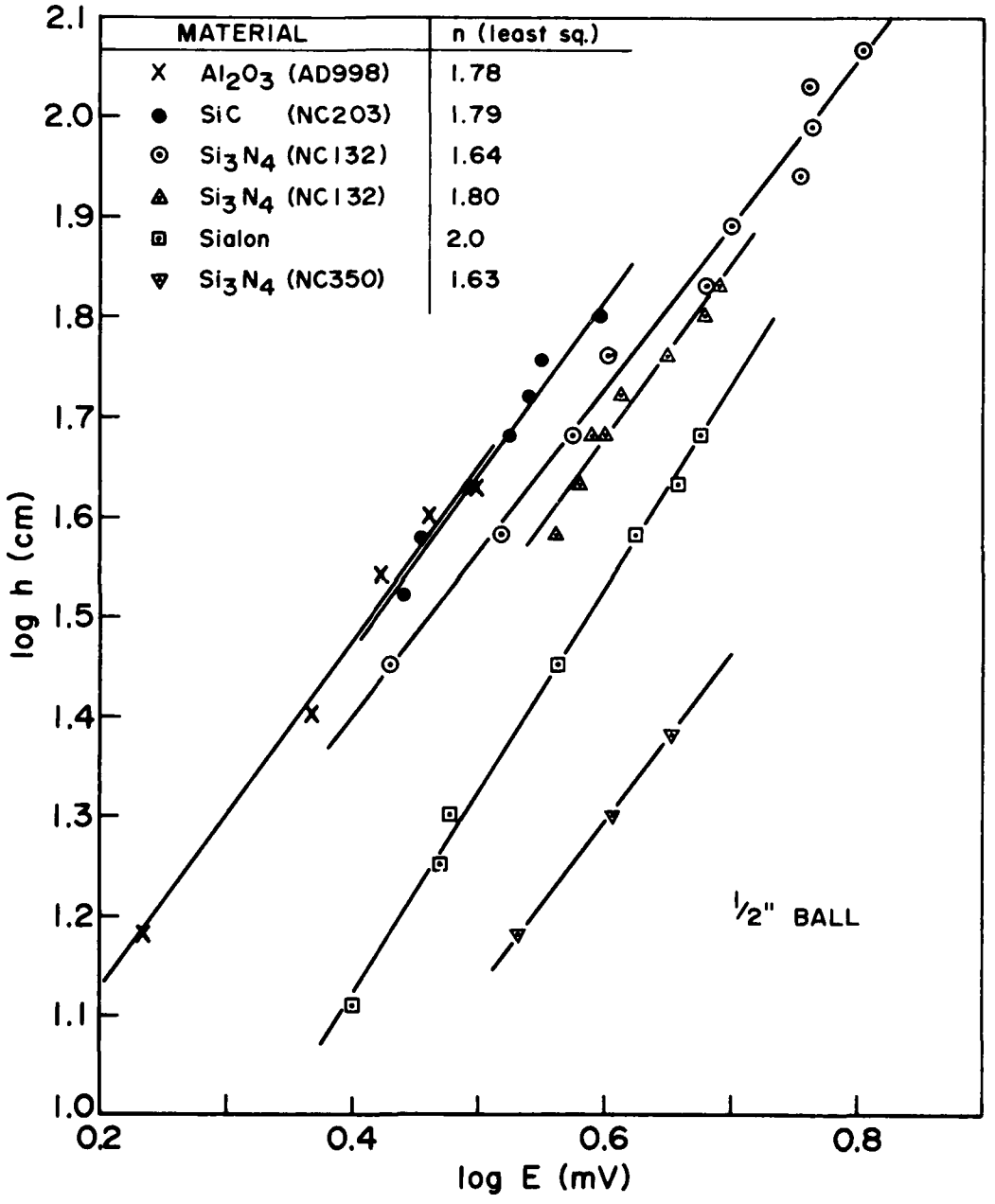

Figure 23. Dependence of Dynamic Stress at Maximum Deflection on h (Ball Size = const.).

SECTION IX

IMPACT FATIGUE

In the DWT, where the specimen sustains several impacts prior to fracture, one might expect to observe strength degredation due to fatigue. The effect of repeated impacts was studied by Smoke,[7] who determined that the fatigue effect is negligibly small or entirely absent. Sarkar and Glinn[8] studied the effect of repeated impacts on "Sintox" Alumina, and found that even at high impact energy loads, close to the single critical impact value, the material endured a minimum of ten impacts without degredation of the single impact strength. Impact fatigue, i.e., strength degredation, might be thought to result from the formation of Hertzian cracks. These cracks will grow conically from the point of contact of the ball and specimen. The critical load required to form Hertzian cracks with 10 mm diameter steel balls is 18×10^4N for ground Al_2O_3 and 2×10^3N for surface-ground self-bonded SiC[9]. The use of a 1/2" ball in the DWT results in loads of the order of 500N, far below the critical load to form Hertzian cracks. Although during a DWT almost all impacts are considerably below the critical level to form Hertzian cracks, the total number of impacts were limited to a maximum of about ten.

To further ascertain the extent of impact fatigue, a NC-203 SiC specimen was impacted 20 times at a stress level 60% of the fracture stress. The specimen was then fractured in a 4-pt bend test with the impact point on the tensile side of the bend test specimen. The 4-pt result was $\sigma_c = 492(MN/m^2)$, in close agreement with the virgin strength of the as-received material (see Table 9). Furthermore, the fracture occurred 4 mm away from the impact point. For the other materials tested no correlation was found between the fracture stress and the number of impacts in the DWT. It is thus concluded that for the limited number of impacts performed in a DWT and their low load levels, fatigue is either negligibly small or absent.

SECTION X

DYNAMIC STRENGTH

1. Dynamic Critical Stress Intensity Factor

According to fracture mechanics considerations, the strength of a ceramic material is determined by the catastrophic propagation of pre-existing flaws when the stress intensity, K_I, reaches a critical value, K_{IC}, in the case of static loading or K_{ID},[10] in the case of dynamic loading. The dynamic strength, $(\sigma_c)_{dyn}$, is related to the static strength, $(\sigma_c)_{stat}$, through the relation $(\sigma_c)_{dyn}/(\sigma_c)_{stat} = K_{ID}/K_{IC}$.

As described in Section VII the instrumented DWT was carried out on specimens of NC-203 SiC using the controlled flaw technique. After fracture the flaw size was measured optically on the fracture surface of specimen 12, and it was found that for that specimen a = 80 μm and 2c = 140μm, where these flaw dimensions are defined as in Fig. 24.

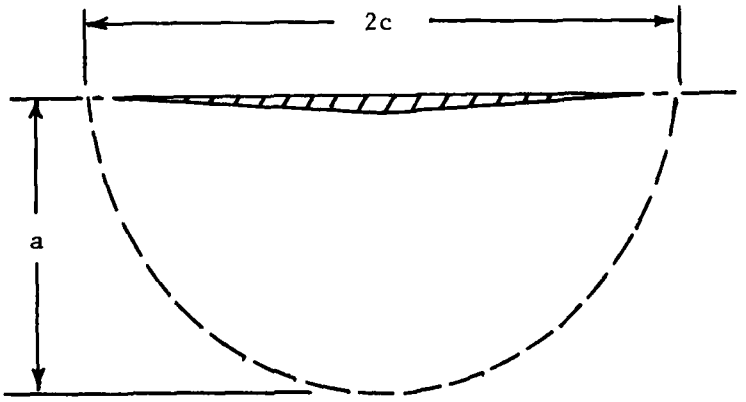

Figure 24. Semi-Elliptical Controlled Flaw, Ref. 3 and 4

K_{ID} was determined from the fracture mechanics relation for a surface flaw under bending:[10]

$$K_{ID} = M\,(\pi a/Q)^{1/2}\,(\sigma_c)_{dyn}$$

Neglecting plastic zone corrections, M and Q are factors which depend on the flaw geometry and on the ratios a/c and a/t where t is the specimen thickness. For the above flaw M = 1.01 and Q = 3.02.[11] Since $(\sigma_{c_2})_{dyn}$ = 250 MN/m^2 for the as-indented NC-203 SiC specimen 12, K_{ID} = 2.3 MN/m^2. The values reported by Petrovik and Jacobson[4] for the same material using the same indenter and load, measured by conventional 4-pt bending tests were K_{IC} = 2.57 MN/m$^{3/2}$ and σ_c = 228.7 MN/m^2. From this single measurement of K_{ID} it appears that at room temperature K_{ID} and K_{IC} are essentially equal. The same result was found on polycrystalline alumina.[12]

Petrovic and Jacobson[4] reported that after the residual stress introduced by the indenter in SiC is removed by annealing at 1400°C in vacuum, K_{IC} increased to 3.8 MN/m$^{3/2}$ and σ_c increased to 415 MN/m^2. The effect of the residual stress can also be removed by grinding.[3] From the instrumented DWT on two ground specimens (see Table 19) it was found that the fracture strength increased only to 300 MN/m^2. One possible explanation for the low value could be insufficient grinding. It is also possible that annealing and grinding have different effects on these specimens.

2. Dynamic Strength at Room Temperature and the Effects of Annealing

In agreement with the above result for NC-203 SiC containing a controlled flaw, i.e., that $K_{ID} \simeq K_{IC}$, it was found for all the ceramics tested that the room temperature dynamic strength determined by the DWT on specimens containing the virgin flaw distribution agreed well with the static strength as determined from 4-pt bend tests. The strength of the as-received NC-132 Si_3N_4 was scattered and had a lower average value than that reported by other investigators.[2] The same observation was also reported by Petrovic et al.[3] These authors attributed the low strength to the edge conditions of the as-received specimens. In fact, no steps were taken either in the present work or in Ref. 3 to eliminate such flaws by bevelling the edges.

An increase in strength of about 60% was observed for as-received NC-132 Si_3N_4 specimens after annealing at 1300°C for one hour in air. Annealing obviously caused some flaw healing.

The 4-pt bend strength of as-received NC-203 SiC specimens was close to the reported values[2] and in agreement with the 4-pt average strength of 480 MN/m^2 reported by Petrovic and Jacobson[4] on as-received specimens from the same source. Also, little scatter was observed both in the 4-pt and the DWT results compared with the scatter of strength measured on as-received NC-132 Si_3N_4. Here also, no attempt was made to eliminate edge flaws. Annealing in air for one hour at 1300°C produced an increase of about 20% in the strength of the as-received specimens, see Table 9.

3. Dynamic Strength at High-Temperature

The dynamic strength at 1300°C for all the ceramics tested was found to be about equal to or greater than the dynamic strength at room temperature. The ceramics NC-132 Si_3N_4, NC-350 Si_3N_4 and Sialon demonstrated somewhat higher dynamic strength at 1300°C than at room temperature.* The actual increase was not determined, since the number of tests was too small to derive a reliable average for the difference in room temperature and high-temperature dynamic strength. Note that the large increase in the dynamic strength of as-received NC-132 Si_3N_4 at high-temperature over the dynamic strength at room temperature is due to annealing in the DWT furnace and that the actual increase of the dynamic strength at high-temperature should be compared with annealed specimens tested at room temperature.

Since the impact time duration is very short, in the range of 150 μs, no crack growth is expected to take place during the time of impulsive loading. In other words, it may be assumed that the flaw distribution in the specimen is frozen during the impact event. It is therefore concluded that K_{ID} (RT) ≃ K_{ID} (HT) for all the ceramics tested. In the case of NC-132 Si_3N_4 this result is in striking contrast to the temperature increase of K_{IC} observed in NC-132 Si_3N_4 by Petrovic et al,[3] where an increase from K_{IC} (RT) = 4.3 to K_{IC} (1300°C) = 9.6 $MN/m^{3/2}$ was reported. The static strength of NC-132 Si_3N_4, however, decreases strongly with increasing temperature due to the onset of slow crack

*The actual high-temperature dynamic strength can in fact be larger by up to a factor of about 1.08 just due to the temperature dependence of the elastic modulus in the Griffith relation.

growth at elevated temperatures. A decrease of about 40% in the bend strength is observed for NC-132 Si_3N_4 at 1300°C[2] compared to the room temperature value. For NC-203 SiC, K_{IC} (RT) = 2.57 $MN/m^{3/2}$ and K_{IC} (1300°C) = 2.0 $MN/m^{3/2}$.[4] The decrease of K_{IC} with temperature for this ceramic is thought to result from a transition from trangranular fracture at room temperature to intergranular fracture at high-temperature. The 3-pt bend strength of NC-203 SiC decreases by about 26% of the room temperature value a 1300°C.[2] For reaction bonded Si_3N_4 the decrease of the static bend strength was found to be about 10% at 1300°C.[2]

The bend strength of both hot-pressed Si_3N_4 and SiC was found to increase with increasing strain rate when deformed above 1200°C.[2] In both cases the stress was found to be proportional to the strain rate in the strain rate range explored (up to about $4x10^{-2}$ sec^{-1} for hot-pressed SiC and 10^{-5} sec^{-1} for hot-pressed Si_3N_4).* These rates are much lower than the strain rates achieved in the DWT (about 20 sec^{-1}). The high-temperature DWT results show therefore that the extension of high-temperature, low strain rate measurements to higher strain rates, as obtained by low velocity impacts, results in dynamic bend strengths equal to or a little higher than the room temperature static (or dynamic) strength.

---

*Measurements are reported in terms of stress rates up to 10^6 $MN/m^2/min$. The DWT provided stress rates in the range $(300-600)x10^6$ $MN/m^2/min$.

SECTION XI

IMPACT RESISTANCE

1. Impact Failure Modes

The failure of brittle materials due to impact is best considered in terms of their achieving the critical stress necessary to initiate the propagation of preexisting flaws. Two distinct failure modes are possible, depending on the level of impact energy. The first is the initiation of crack growth due to localized Hertzian stresses at the projectile-ceramic interface. These cracks propagate conically and can give rise to strength degradation or even catastrophic fracture. The second results from longer range stresses, caused by the elastic deflection of the impact body. These stresses are frequently flexural and will cause, in sufficiently flexible geometries, catastrophic fracture initiated in a tensile region.

In the present work the experiments were designed so that the impact resistance to flexural stress was studied by the DWT. For the geometry used, the loads exerted by the impactor were below the level required for the formation of Hertzian cracks. The effect of Hertzian cracks were studied in ballistic tests, where the impulsive loading due to the high velocity impactor was over an order of magnitude higher than in the DWT.

2. Impact Resistance and Impact Fracture Energy for Flexural Dynamic Loading

A clear distinction should be made between the energy loss of an impactor in an impact test (the pendulum in a Charpy test or the ball in a DWT) and the actual energy consumed in the sample during fracture. The first energy is sometimes referred to as the "Impact Resistance" and is the outcome of the common uninstrumented Charpy test. The second energy is referred to as the "Impact Fracture Energy". Unlike metals, ceramics do not absorb significant amounts of energy by plastic deformation. As a result: 1) the Impact Fracture Energy of ceramics is much lower than that of metals, and 2) the Impact Fracture Energy is essentially the elastic energy stored in the sample at

fracture, i.e., $(EE)_c$, since the energy for formation of new surface is just a few percent of the stored elastic energy at fracture. It has already been pointed out by several investigators that the Impact Fracture Energy is only a small part (8-30 pct) of the Impact Resistance energy as determined in uninstrumented Charpy tests. The latter energy depends, to a large extent, on the impact machine compliance, tup velocity, toss energy (i.e., the kinetic energy imparted to the specimen) and other impact machine losses,[12] and, therefore, cannot be used as a reliable measure of the true impact resistance of the material itself. In the present DWT, high values of this energy were found (see Table 21) due to minimizing: 1) energy loss to the machine and 2) toss energy due to the incremental impact energy approach. The only material dependent impact property is the Impact Fracture Energy, which can be determined only from instrumented impact tests such as the instrumented Charpy test and the instrumented DWT. The Impact Fracture Energy of a ceramic is determined by its dynamic strength. At room temperature, where an entirly brittle fracture occurs, it is reasonable that the dynamic strength is about the same as the static strength and the Impact Fracture Energy can be derived using σ_c (static) in $(EE)_c = V\sigma_c^2/18E$. At high-temperature, however, where plasticity or slow crack growth are present, the static strength can be much lower than the dynamic strength obtained at very high strain rates, and, therefore, the calculation of the Impact Fracture Energy based on the high-temperature static strength may give an erroneous result. The actual value can only be obtained from instrumented impact tests at high-temperature.

3. Screening Ceramics for Dynamic Strength and Impact Resistance

As discussed earlier the only relevant measure of impact resistance when the failure is due to flexural stress is the Impact Fracture Energy, $(EE)_c$, given for a beam as: $(EE)_c = V\sigma_c^2/18E$. In other words, $(EE)_c$ is the minimum energy that the projectile has to deliver to the specimen in order for the stress to reach the dynamic strength. Thus, if $(EE)_c$ is used to screen ceramics for impact resistance to flexural stresses, then $(\sigma_c^2)_{dyn/E}$ is the parameter which defines this property of the ceramic. In Table 22 the average dynamic strength and the parameter $(\sigma_c^2)_{dyn/E}$ of the tested ceramics is given along with their ratio to NC-132 Si_3N_4.

Table 22: Summary of Dynamic Strength and Impact Resistance Parameter and Comparison to NC-132, Si_3N_4

Material	σ_c (MN/m^2)		σ_c^2/E (MN/m^2)		$(\sigma_c)/(\sigma_c)_{NC-132}$		$\left(\frac{\sigma_c^2}{E}\right) \Big/ \left(\frac{\sigma_c^2}{E}\right)_{NC-132}$	
	RT	1300°C‡	RT‡	1300°C‡	RT	1300°C	RT	1300°C
Si_3N_4* (NC-132)	685	785	1.81	2.25	1	1	1	1
SiC* (NC-203)	525	505	0.72	0.62	0.77	0.64	0.40	0.28
Si_3N_4 (NC-350)	330	455	0.62	1.17	0.48	0.58	0.34	0.52
Al_2O_3 (AD 998)	390	390	0.37	0.32	0.57	0.50	0.20	0.14
Sialon	385	490	0.66	1.04	0.56	0.62	0.36	0.46
SiC§ (NC-435)	355	420	0.44	0.62	0.52	0.54	0.24	0.28

*Annealed

‡Calculated from Eq. 5 using RT values of E and α_{av}

‡Calculated from $(\alpha)_{av}(mgh_c)_{av}$, assuming $\alpha \neq f(T)$

§The data on this material was scattered and, therefore, the values quoted in Table 22 might be subject to large variations.

The conclusion from the results in Table 22, is that while the dynamic strength of two materials may differ by less than a factor of two, their impact resistance can differ considerably. For example, the high-temperature dynamic strength ratio of NC-132, Si_3N_4 to NC-203, SiC is only about 1.5, while the ratio of their impact resistance parameters is 3.6.

Improvements in impact resistance can be achieved by increasing the dynamic strength since the impact resistance parameter is proportional to σ_c^2. However, at this stage of material development, strength improvements greater than a factor of two are not anticipated. As a result, improvement in impact resistance by a factor of 4-5 is the maximum that can be achieved. Other approaches such as composite materials have been suggested but these remain to be proven.

REFERENCES

1. S. J. Aquaviva, "A Drop-Weight Test for the Impact Strength of Ceramic Materials", Materials Resch. and Standards, 21, 11 (1971).

2. J. W. Edington, D. J. Rowcliffe and J. L. Henshall, "The Mechanical Properties of Silicon Nitride and Silicon Carbide. Part I: Materials and Strength", Powder Metall. Intern. 82, 7 (1975); "Part II: Engineering Properties", Powder Metall. Intern. 136, 7 (1975).

3. J. J. Petrovic, L. A. Jacobson, P. K. Talty and A. K. Vasudevan, "Controlled Surface Flaws in Hot-Pressed Si_3N_4", J. Am. Ceram. Soc., 58, 113 (1975).

4. J. J. Petrovic and L. A. Jacobson, "Controlled Surface Flaws in Hot-Pressed SiC", J. A. Ceram. Soc., 59, 34 (1976).

5. W. Goldsmith, "Impact", Edward Arnold Publ. Ltd., London, 1960.

6. S. Timoshenko and J. N. Goodier, "Theory of Elasticity", McGraw-Hill Book Co., N. Y. 1951, pp. 383.

7. "Inorganic Dielectric Research", R&D TR ECOM-023205 Rutgers University, N. J. Dec. 1969.

8. B. K. Sarkar and T. G. J. Glinn, "Impact Fatigue of an Alumina Ceramic", J. of Materials Science, 951, 4, 1969.

9. A. G. Evans, "Strength Degredation by Projectile Impact", J. Am. Ceram. Soc., 56, 405(1973).

10. A. G. Evans, "Structural Ceramics" (Preprint), Progress in Materials Science (1975) to be published.

11. R. H. Keays, "Review of Stress Intensity Factors for Surface and Internal Cracks", Structures and Materials Dept. 343, Department of Supply, Australian Defense Scientific Service, Aeronautical Research Laboratories, April 1973.

12. R. L. Bertolotti, "Strength and Absorbed Energy in Instrumented Impact Tests of Polycrystalline Al_2O_3, " J. Am. Ceramic Soc., 57, 300 (74).

13. R. L. Bertolotti, "Fracture Toughness of Polycrystalline Al_2O_3", J. Amer. Ceramic Soc., 56 (2) 107 (1973).

14. R. W. Davidge and D. C. Phillips, "The Significance of Impact Data for Brittle Non-Metallic Materials", J. of Materials Science, 1308, 7 (1972).

15. H. P. Kirchner, R. M. Gruver and W. A. Sotter, "Use of Fracture Mirrors to Interpret Impact Fractures in Brittle Materials", J. Amer. Ceram. Soc., 58, 188 (1975).

16. E. Wysong, I. Bransky and N. M. Tallan, "Determination of Dynamic Strength and Impact Resistance from Instrumented Impact Tests on Ceramics up to 1320°C", to be published.